Second Edition

The Environmental Chemistry of Aluminum

Edited by Garrison Sposito, Ph.D.
Department of Environmental Science,
Policy, and Management
University of California
Berkeley, California

LEWIS PUBLISHERS

Boca Raton New York London Tokyo

Library of Congress Cataloging-in-Publication Data

The environmental chemistry of aluminum / edited by Garrison Sposito.
-2nd ed.
p. cm.
Includes bibliographical references and index.
ISBN l-56670-030-2 (alk. paper)
1. Aluminum-Environmental aspects. 2. Water-Pollution. 3. Soil-pollution.
I. Sposito, Garrison, 1939-
TD427.A45E58 1995
628.5'26--dc20 9520082
CIP

Lewis Publishers is an imprint of CRC Press

No claim to original U.S. Government works
International Standard Book Number o-87371-030-2
Library of Congress Card Number 95-20082
Printed in the United States of America 1 2 3 4 5 6 7 8 9 0
Printed on acid-free paper

CHAPTER 7

The Surface Chemistry of Aluminum Oxides and Hydroxides

Sabine Goldberg, James A. Davis, and John D. Hem*

CONTENTS

* Deceased December 26, 1994

1-8737-1030-2/96/$0.00+$.50

I. INTRODUCTION

The coordination behavior of Al^{3+} toward hydroxide ions explains the marked dependence of aluminum hydroxide solubility on pH. The ratio of the ionic radii favors octahedral coordination, with Al^{3+} at the center of an octahedron formed by six close-packed hydroxide ions (compare Figure 1 in Chapter 2). The water molecule, OH^-, and O^2- ions all have nearly the same physical dimensions and can replace each other in some crystal structures. A crystal structure is broken or cleaved along preferred crystal planes where the structure is weakest, creating the surface of the mineral. Thus, the initial surface structure can be related to the crystal structure and the way in which the surface was formed. Furthermore, the surface chemical behavior of aluminum oxides and hydroxides can be explained in part by surface structure expected for particular crystals. Complications may arise, however, if the surface is altered by exposure to water or changes in environmental conditions.

The general physical properties of various forms of aluminum oxides and hydroxides are reviewed in Chapter 3 and elsewhere.[1-3] In this chapter, we review the surface chemical behavior of these oxides and hydroxides, with an emphasis on adsorption studies and the electrochemical behavior of the alumina-water interface. When possible we have contrasted the observed behavior of different crystal forms in terms of what is known about their surface structure. The hydroxides and oxyhydroxides of aluminum are probably the more important phases in terrestrial systems.^2 However, most of the data on surface chemical behavior are available from studies of the crystalline hydroxide, gibbsite [α-$Al(OH)_3$], or the synthetic oxide, γ-Al_2O_3, although limited information is available for other phases. We also present a discussion of crystal formation for various phases and the ways in which surface chemical behavior may influence the final precipitate formed.

This discussion is limited to the relatively pure and well-crystallized oxide and hydroxide species and considers the mechanism of their formation during precipitation from the standpoint of the "gibbsite fragment" hypothesis. The topic of hydroxide polymerization is discussed more fully in Chapter 4 of this volume and has been reviewed by May.' The phase discontinuity that occurs at the alumina-water interface may play an important role in the geochemical processes occurring in soils. The composition of soil solutions and the flux of solutes through soils are often controlled by reactions at

the mineral-water interface," and the surfaces of aluminum oxides and hydroxides are particularly reactive in comparison to other minerals in the soil environment. Probably one of the most important topics in this context is the geochemical control of dissolved phosphate in soil solutions because of the commercial importance of phosphate as a nutrient. The rate of delivery of phosphate and other nutrients to plant roots may be controlled in some soils by processes that occur on the surfaces of aluminum oxides and hydroxides (see Chapter 8).

II. RELATIONSHIP OF CRYSTAL STRUCTURE TO SURFACE CHEMISTRY

A. SURFACE FUNCTIONAL GROUPS

All strongly dried aluminum oxides and hydroxides chemisorb at least a monolayer of water when exposed to moisture at room temperature. Figure 1 shows the idealized structure of a γ-Al_2O_3 surface when dried and when exposed to water." When dry, the top layer contains only oxide ions, regularly arranged over aluminum ions in octahedral sites in the lower layer (Figure la). This upper layer contains only half of the oxide ions present in the next lower layer, which represents the 100 plane of a cubic, close-packed oxide lattice, where each oxide ion occupies an area of 0.08 nm^2. Aluminum ions are located in all interstices between oxide ions. The stoichiometry of the upper two layers combined corresponds to Al_2O_3. When the surface is hydrated, water is chemisorbed to convert the top layer of oxide ions to a filled, square lattice of hydroxyl ions (Figure 1 b). Each hydroxyl ion is assumed to be directly over an aluminum ion in the next lower layer. In the hydrated form, the two upper layers correspond stoichiometrically to $Al_2O_3 \cdot H_2O$.

Hydroxyl ions coordinated in various ways with aluminum cations constitute the reactive functional groups of alumina surfaces. In general, more than one kind of surface OH group can be distinguished on the basis of stereochemical reasoning, and these different groups have properties (e.g., their infrared [IR] absorption spectra) that set them apart from OH groups inside the bulk mineral structure.[7] The number and type of each surface OH group depend on which crystal planes are exposed preferentially and how aluminum ions are distributed at the surface. For example, cleavage of gibbsite crystals occurs preferentially along the 001 planes, since this involves only the breaking of relatively weak hydrogen bonds which hold the layers of the structure together. The surface hydroxyl ions in this plane would appear as a close-packed, pseudo-hexagonal array, with each OH coordinated to a pair of underlying aluminum ions. This basal plane makes up most of the surface of gibbsite. At the edge faces (100 and 110 planes), aluminum ions with potentially unsatisfied positive charge may be exposed. At such sites, hydroxide ions can be present that are, in effect, coordinated by only one aluminum ion and these groups are more reactive, as will be discussed below in more detail.

B. GIBBSITE, α-$Al(OH)_3$

The crystal structure of gibbsite, the most common of the $Al(OH)_3$ minerals, has been modeled in a number of ways. One simple model uses spheres of two different

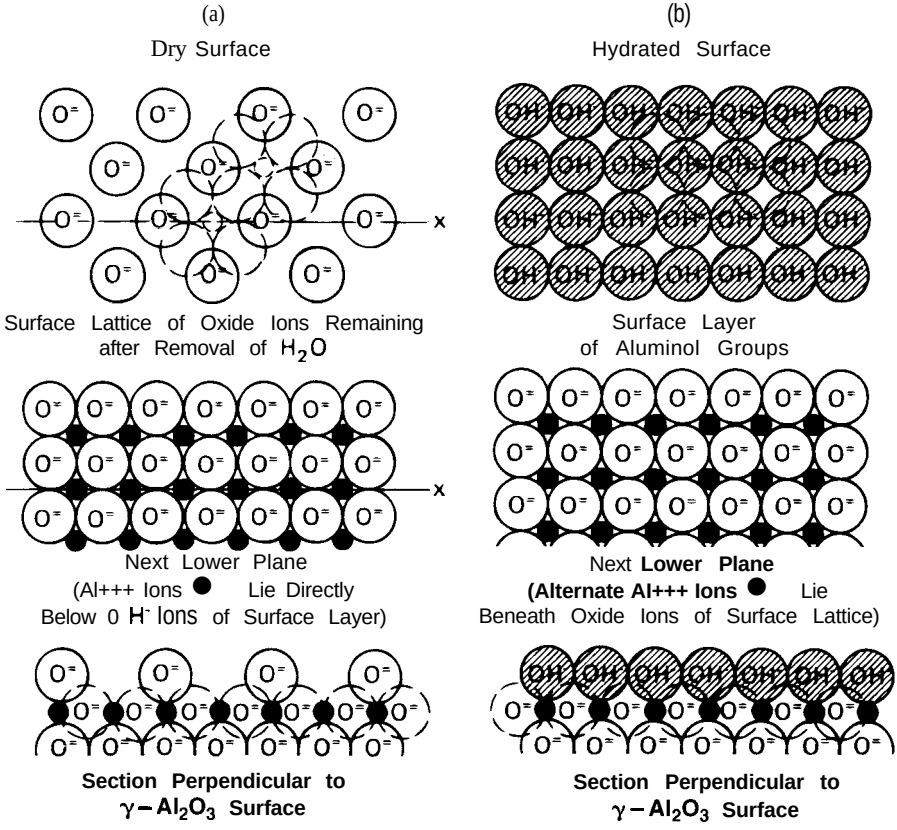

Figure 1 Idealized illustration of the dry and hydrated surface of γ-Al_2O_3. (Modified from Peri, J. B., J. *Phys. Chem., 9,* 220, 1965.)

sizes. The larger spheres, representing OH- ions, are arranged in a close-packed double-layer structure with the smaller spheres, representing Al^{3+} ions, occupying interstices between the two OH layers. Two types of interstices (i.e., cation sites) occur in this structure. The smaller, tetrahedral sites are surrounded by four of the large spheres, three in one layer and one in the other. The larger, octahedral sites are surrounded by six of the larger spheres, three in each layer. Figure 2 is a sphere model of a segment of the gibbsite structure with part of the upper hydroxide layer removed to show the arrangement of Al^{3+} ions. An electroneutral structure is achieved when Al^{3+} ions occupy only two thirds of the octahedral sites (i.e., dioctahedral arrangement). The Al^{3+} ions are coordinated to six OH^- ions with each OH^- ion shared with two Al^{3+} ions. This results in the orderly arrangement shown in Figure 2. Crystal growth occurs by extension in the plane of the layer structure (a and b directions) and by vertical stacking of these layers (c direction).

The surface hydroxyls of an ideal gibbsite basal plane may be coordinated to two Al^{3+} ions while edge plane hydroxyls are coordinated to one Al^{3+} ion. Parfitt et al.[8] estimated that the basal plane of gibbsite contains approximately I2 hydroxyl groups

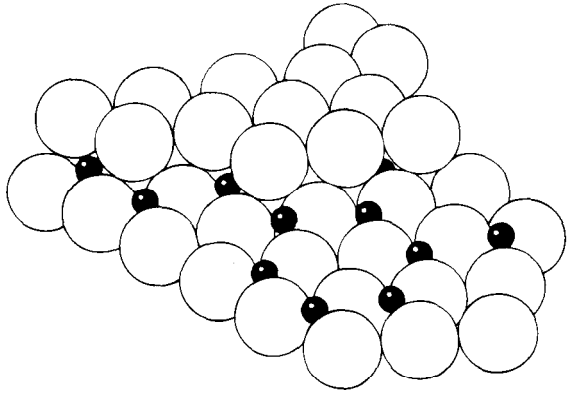

Figure 2 Sphere model of gibbsite structure. Large spheres represent OH^- ions, smaller spheres represent Al^{3+} ions in octahedral coordination sites. Part of upper OH layer removed to show arrangement of Al^{3+}.

per square nanometer of surface while edge planes contains about 4 groups per square nanometer.

The structure of gibbsite can also be viewed from the perspective of the Al^{3+} ions, which are arranged in a pattern of coalesced hexagonal rings. A single ring of six Al^{3+} ions, joined above and below by six pairs of bridging OH^- ions, is the smallest recognizable unit of the gibbsite structure. Figure 3a represents the ring with the upper hydroxide

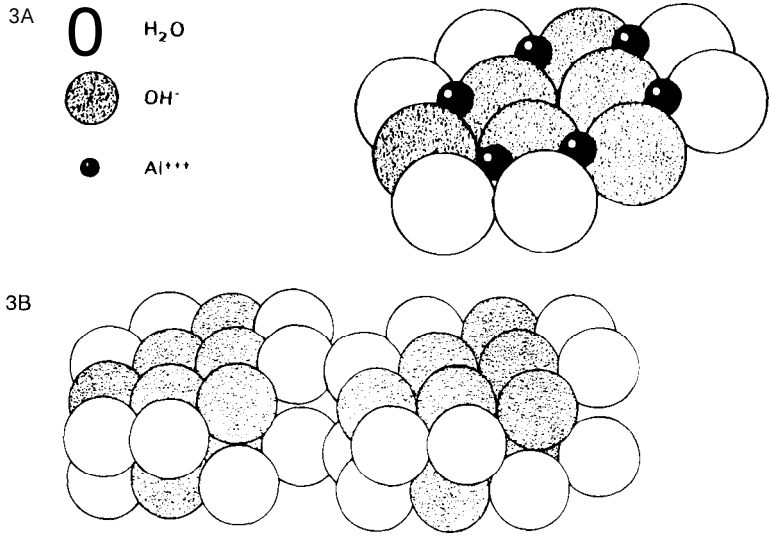

Figure 3 Sphere model of polymeric ion $Al_6(OH)_{12}(H_2O)_{12}^{6+}$. (A) Single ion with upper $OH^- + H_2O$ layer removed to show arrangement of Al^{3+} ions (small dark spheres). (B) Two complete ions. White spheres represent H_2O molecules, shaded spheres represent OH

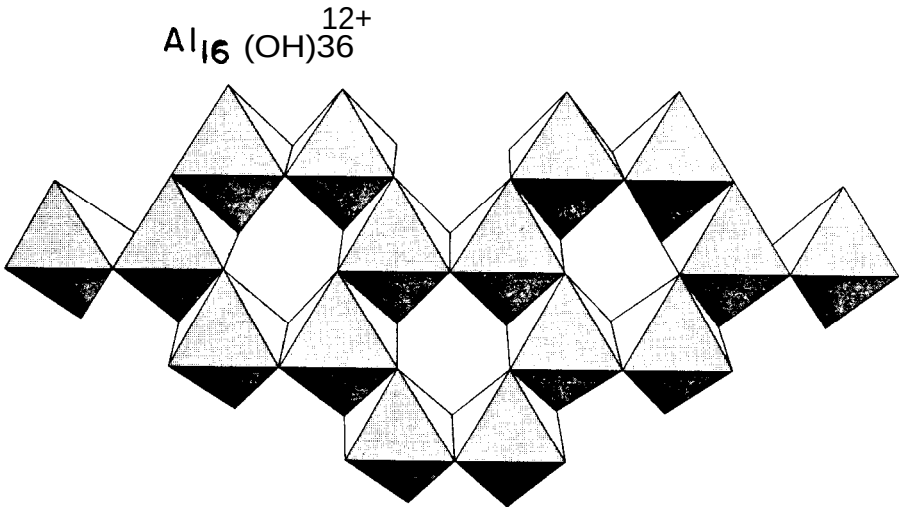

Figure 4 Octahedral model of gibbsite structure consisting of three coalesced $Al_6(OH)_{12}$ rings with two additional aluminum ions.

layer removed to show the locations of Al^{3+} ions. A sphere model of two six-membered rings is shown in Figure 3b. The shaded spheres in this model are OH- ions and the clear ones are H_2O molecules. The excess positive charge on each Al^{3+} ion retains a pair of H_2O molecules, shown in the model to be inclined at an angle of 60" to the face of the ring structure. Two rings can be joined by replacing inclined pairs of H_2O molecules on adjacent rings with two bridging OH^- ions.

Alternatively, the $Al(OH)_6$ unit can be represented schematically as an octahedron, with each apex being at the center of an OH ion. Two octahedra are joined along one edge by sharing a pair of OH ions, i.e., $Al(OH)_2Al^{4+}$. Six octahedra, each sharing two edges, yield an $Al_6(OH)_{12}^{6+}$ ring. This model depicts the three-dimensional gibbsite crystal structure as an array of octahedra sharing three edges, to form the pattern shown in Figure 4. The shared edges represent pairs of bridging OH^- ions. The apparent "holes" in the structure in Figure 4 stress the dioctahedral arrangement of Al^{3+} ions in the structure.

Another way of representing gibbsite structures in two dimensions is shown in Figure 5. The double OH bridges in Figure 5a are represented in the other structures by straight lines describing hexagons with Al^{3+} ions at each corner. The rings, in turn, are joined by formation of additional OH bridges, represented by dashed lines, joining the corner Al^{3+} ions and giving polymeric ions with the formulas and physical dimensions noted in the illustration. If the polymer growth process is based on coalescence of $Al_6(OH)_{12}^{6+}$ rings (compare Chapter 4), the geometry of the units is constrained by the requirement that two complete ring units cannot combine with each other by sharing hexagonal edges, but must join at corners (i.e., octahedral edges) by establishing additional $(OH)_2$ bridges.

The structural model proposed for gibbsite (Figures 2 to 5) suggests that Al^{3+} ions located at the corners of $Al_6(OH)_{12}$ rings will have one unsatisfied positive charge. Two water molecules could be retained in coordination positions at such sites. Attachment of another ring at that site entails deprotonation of two of the four H_2O molecules

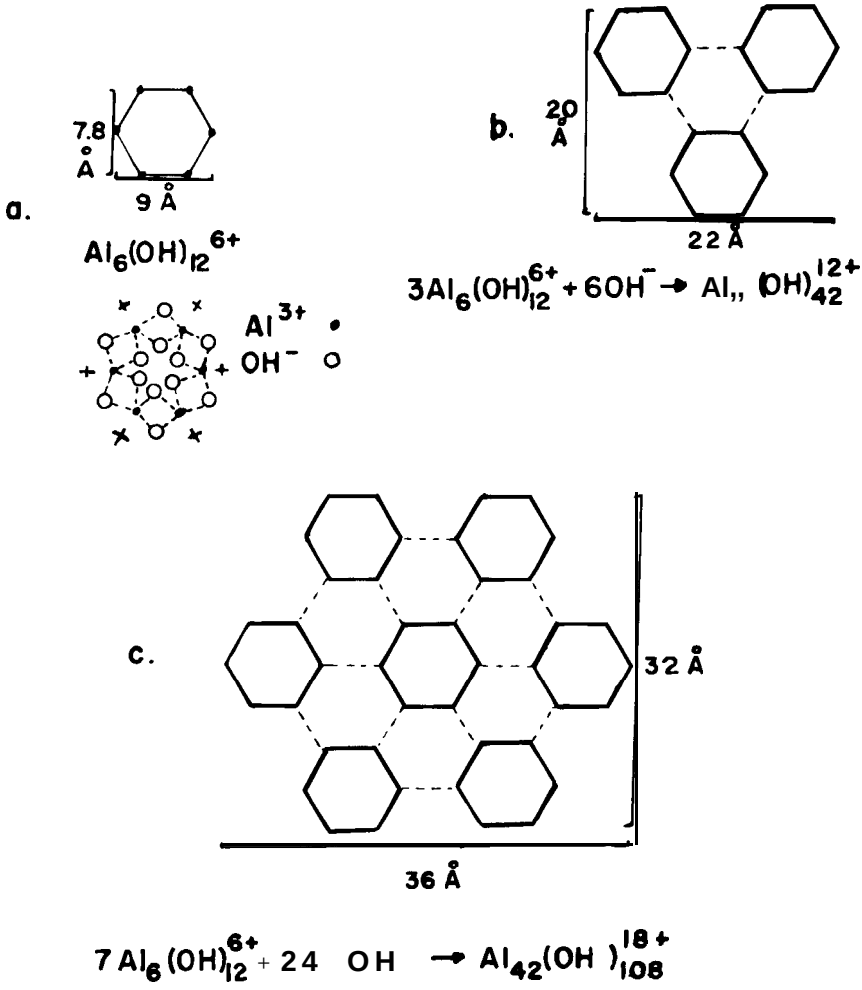

Figure 5 Two-dimensional representations of aluminum hydroxide structures and approximate dimensions in Angstroms. (a) $Al_6(OH)_{12}$ ring shown in two different ways-with OH^- double bridges drawn in (not to scale) and with bridges represented by straight lines connecting Al^{3+} ions. (b) Four-ring polymer, formed from three independent $Al_6(OH)_{12}^{6+}$ units joined by three additional double OH^- bridges (dashed lines). (c) 13-ring polymer formed from seven independent six-membered rings joined by 12 double OH bridges (dashed lines).

involved and release of the other two into solution. At higher pH, the coordinated water molecules might be replaced by a single OH-. This condition would tend to inhibit lateral growth of the gibbsite structure.

The corner charge sites described above constitute aluminol groups (AlOH) or surface hydroxyl sites that will be described below. Another possible form of edge Al^{3+} ions is represented diagrammatically in Figure 4. This structure comprises three $Al_6(OH)_{12}$

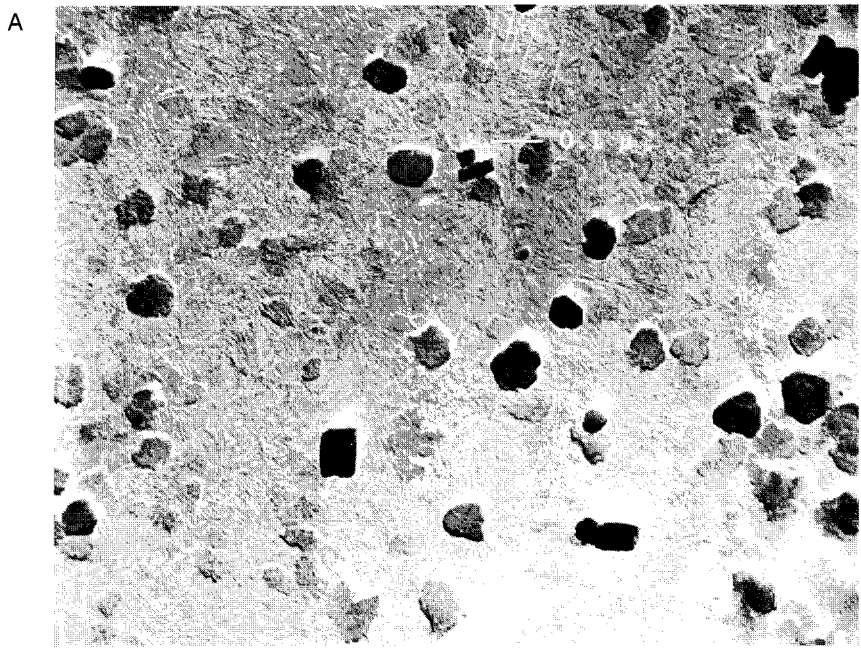

Figure 6 Transmission electron micrographs of aluminum hydroxide precipitates: (A) gibbsite, (B) bayerite, (C) bayerite and nordstrandite (rectangles).

rings, with two additional aluminum octahedra that are attached to the structure through single (OH), bridges. If the edges of gibbsite crystals actually include Al^{3+} ions that are not part of a ring structure, then these two Al^{3+} ions could represent potential adsorption sites with double positive charges.

Defects and elemental substitutions in the gibbsite crystal structure may lead to a net charge imbalance. At the surface, where the crystal structure is abruptly truncated, electroneutrality is achieved by adsorption of ions or molecules at empty or incompletely filled coordination sites. Both positive and negative charge sites may exist on the crystal faces. However, where defects or layer growth sites are absent, the charge density on crystal faces will be substantially less intense than those at crystal edges or corners. Electron micrographs of synthetic gibbsite crystals bearing adsorbed particles of a negatively charged gold sol illustrate this phenomenon rather strikingly." The gold sol particles are generally attached to crystal edges, corners, and imperfections. Another example is shown in Figure 6a, an electron micrograph of gibbsite particles produced by slow addition of OH to a dilute $Al(ClO_4)_3$ solution ($<10^{-4}$ mol dm^{-3}) maintained at pH 5.4 and 25°C. The particles display different amounts of layer stacking and various types of surface irregularities that could produce favorable sites for adsorption. McBride et al.[10] have also observed the occurrence of crystal steps at regular intervals on gibbsite plates.

C. γ-Al_2O_3

Although gibbsite is probably the most important aluminum-bearing oxide mineral in soils and sediments, more is known about the surface chemistry of γ-Al_2O_3 than

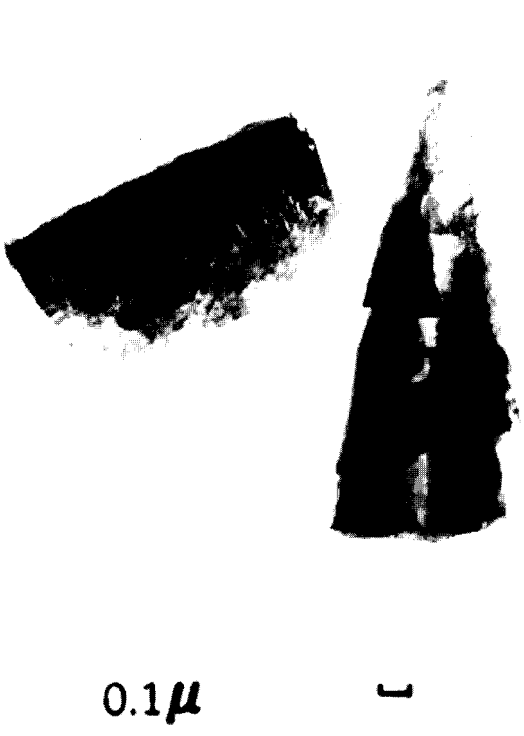

Figure 6 *continued*

gibbsite because of the significance of γ-Al_2O_3 as a catalyst in industry. Electron and X-ray diffraction studies indicate that γ-Al_2O_3 may preferentially expose the 100 plane of the defect spine1 lattice. The surface of γ-Al_2O_3 is hydroxylated when water chemisorbs and combines with oxide ions which have broken bonds along the cleavage plane (Figure 1). The hydrated surface retains 12.5 molecules of water per square nanometer of surface after evacuation at 25°C for 100 h.[11] Although most of the water is chemisorbed and held in hydroxyl groups, IR studies suggest that some of the water strongly adsorbed at 25°C remains as molecular water. Kummert and Stumm[12] reported a value of 8.5 exchangeable protons per square nanometer on γ-Al_2O_3 using the isotopic exchange technique of Yates and Healy.[13] This value is about one third of that expected on the basis of results from Peri and Hannan.[11] Other authors have attempted hydroxyl group determinations from acid-base titrations in water. These methods yield significantly lower values (e.g., 1.3 protons per square nanometer by Kummert and Stumm[12]) because of incomplete ionization of hydroxyl groups.

In the idealized model of the hydrated alumina surface presented in Figure 1, two types of surface hydroxyl group can be distinguished: those coordinated with one aluminum ion and those coordinated by two aluminum ions. The singly coordinated groups are more basic and more likely to participate in ligand exchange reactions. Since the hydroxyl groups on the edge planes of gibbsite may also be singly coordinated, one may expect some correlations of the surface chemistry of γ-Al_2O_3 with that of the edge faces of gibbsite. It would be useful to know if this hypothesis is true, since a significant number

C

Figure 6 continued

of surface chemistry studies have been conducted with γ-Al_2O_3. These studies then would also be useful in modeling the chemistry on the edge faces of gibbsite. Since the faces are more reactive than the basal planes of gibbsite, it is probably more important to understand the chemical behavior of the edge faces than that of the basal planes.

In comparing the behavior of one γ-Al_2O_3 sample with another, one should ostensibly normalize the reactivity in terms of surface area. For example, one may compare the maximum adsorption of a specific solute or its energy of adsorption per unit surface area. However, this approach is probably inappropriate when comparing the reactivity of one type of aluminum oxide with another. The unique nature of the crystal faces means that the reactivity of the surface cannot be normalized on the basis of the total surface area. The reactivity of each face should be considered separately.

D. OTHER $Al(OH)_3$ POLYMORPHS

Two other minerals, bayerite and nordstrandite, have the composition $Al(OH)_3$ and differ in structure from gibbsite only in the way that the double layers of coordinated OH^- and Al^{3+} are stacked to form the three-dimensional crystal units. Bayerite and nordstrandite were first discerned in synthetic material, but were later found to occur naturally." They are relatively rare, however, in natural material (see Chapter 3).

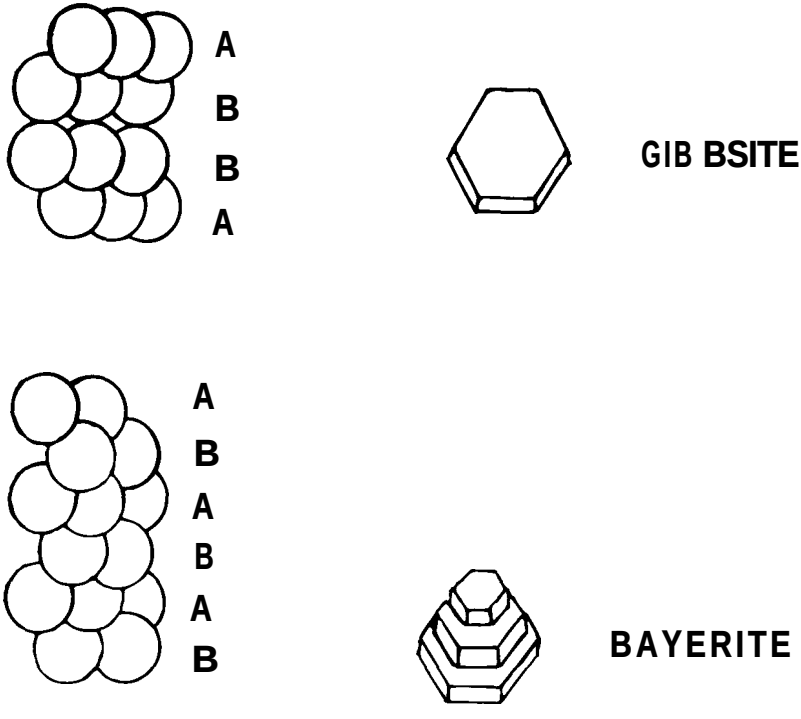

Figure 7 Gibbsite and bayerite layer stacking patterns.

During the synthesis of gibbsite from dilute $AlClO_4$ solutions near pH 5.0, it appears that some critical size of individual sheet structures is attained before a significant amount of growth through stacking of layers takes place.[15] The crystals seen in electron micrographs are fairly uniform in size and the number of layers is generally not large; thus, the crystals appear predominantly as hexagonal plates. However, at pH values above that of minimum gibbsite solubility, growth in the c direction appears to occur more readily through stacking of the gibbsite sheets. As will be discussed later, this pH dependence may be caused by the development of electrical charge on the surface. Bayerite, precipitated near pH 9.0 (Figure 6b) displays a layered crystal habit. Units seen in electron micrographs are generally oriented with their c axis in the plane of the photograph and usually have a conical or barrel-shaped appearance. Another polymorph found at higher pH is nordstrandite, which generally appears as elongated rectangular shapes in electron micrographs (Figure 6c).

Schoen and Roberson[14] explained the change in crystal habit as related to the way the layers of OH^- ions are stacked. In gibbsite (Figure 7) the OH- ions of the upper layer are directly above those in the lower layer, giving an "open packing" arrangement. Bonding between layers was thought to be related to distortion of hydroxyl ions in the vicinity of Al^{3+} ions, compared to ions in other parts of the lattice. In the bayerite structure the OH^- ions of adjacent layers interdigitate (Figure 7). Presumably, at higher pH the effect of coordinated Al^{3+} in the structure is weaker and the ionic species of aluminum in solution that enters the growing structure becomes predominantly anionic

$Al(OH)_4^-$. In nordstrandite the structure can be considered a combination of alternate gibbsite and bayerite layering patterns.

E. α-Al_2O_3 (CORUNDUM)

Corundum occurs naturally as an igneous and metamorphic mineral and is synthesized artificially by various high-temperature techniques. The crystal structure of corundum is described by Wefers and others[3,16] as a hexagonal close-packing of oxygen ions with Al^{3+} ions occupying two thirds of the octahedral interstices. In effect this structure could be visualized as composed of alternating layers of O^{2-} ions and Al^{3+}. Thus, interlayer bonding between aluminum and oxygen is well established in the *c* direction as well as in the *a* and *b* directions. It is to be expected that the surface properties of different crystal faces of corundum will be similar. However, the mode of preparation of synthetic material may affect the distribution of crystal defects. The surface hydroxyl density of α-Al_2O_3 (corundum) has been estimated as six groups per square nanometer by Smit and Holten,[17] from crystal lattice considerations.

F. γ-AlOOH (BOEHMITE)

Boehmite is a common mineral with the composition AlOOH. It is present in some bauxites, especially those of the Mediterranean region.' The processes by which boehmite is produced in bauxite deposits in preference to gibbsite are not well understood. Sphere models of the crystal structure of boehmite are given by Wefers and Bell,[16] who describe the structure as composed of double layers of oxygen and hydroxide in cubic packing. As in gibbsite, the double layers are joined by hydrogen bonds, and crystals exhibit preferential cleavage in the direction perpendicular to the genera1 direction of the hydrogen bonding. Aluminum oxyhydroxide structures have some similarities with those of iron oxyhydroxides and, therefore, a significant amount of Fe^{3+} can replace Al^{3+} in the boehmite crystal lattice. DeBoer et al.[18] determined the hydroxyl group density on γ-AlOOH (boehmite) from IR studies as 16.5 groups per square nanometer.

G. α-AlOOH (DIASPORE)

Diaspore is a naturally occurring mineral that is a major constituent in some bauxite ores and in certain aluminum-rich clays and metamorphic rocks.[3] Thermodynamic data given by Robie et al.[19] indicate that the standard Gibbs free energy of formation of diaspore is 3.6 kJ more negative than that of boehmite. Studies of the crystal structure of diaspore quoted by Wefers and Misra[3] indicate that the aluminum ions are in a somewhat distorted octahedral coordination with the 0" and OH^- ions in the crystal.

III. SURFACE ACIDITY AND THE ELECTRICAL DOUBLE LAYER

A. ACIDITY OF THE DEHYDRATED ALUMINA SURFACE

The surface acidity (ability to release protons from surface sites) of aluminum oxides is of long-standing interest, for both practical and theoretical reasons. The acidic

properties of γ-Al_2O_3 have been of particular interest, because it is widely believed that the catalytic properties of this material are related to the density and type of acidic sites.'" A variety of methods has been used to investigate the relative acidity of hydroxyls on alumina surfaces, including direct titration with acid-base indicators,[20–24] IR spectroscopy>[21,24–28] and nuclear magnetic resonance (NMR) spectroscopy.[29,30] However, these techniques generally have examined the acidity of functional groups on the alumina surface after dehydration at elevated temperatures in a vacuum. As shown by Peri,[6,31] most surface hydroxyls are removed by evacuation at temperatures greater than 400°C, but distinct types of hydroxyls are left on the surface instead of hydroxyls at random sites. The relationship between the acidity of groups remaining on the dehydrated surface and that of the hydrated surface remain obscure. "Strain" sites are created by the process of dehydration at high temperature and some of these sites exhibit considerable acidity. A portion of the sites are produced by the creation of strained Al-O-Al linkages, but other types of site must also develop during dehydration."

B. ACIDITY OF THE HYDRATED ALUMINA SURFACE

The hydroxylation of oxide surfaces is complete at 25°C for relative humidities well below 1%.[32] In the idealized model presented in Figure 1, two types of surface hydroxyl group were distinguished: those coordinated with one aluminum cation and those coordinated by two aluminum cations. The doubly coordinated hydroxyl groups are expected to be more acidic because of the strong polarization induced by the aluminum ions on the oxygen atom." The singly coordinated hydroxyl groups should be less acidic in nature. The hydrated alumina surface exhibits amphoteric behavior in water, i.e., it is capable of adsorbing or releasing protons. This behavior has been attributed generally to amphoteric surface hydroxyl groups instead of independent basic and acidic surface groups.'" For a hypothetical system consisting only of pure water and an immersed alumina surface, the ionization reactions of the surface hydroxyl (aluminol) groups can be described in the following way:

$$AlOH + H^+ = AlOH_2^+ \quad (1)$$

$$AlOH = AlO^- + H+ \quad (2)$$

where AlOH represents an aluminol group. These reactions lead to the development of electrical charge and potential on the surface. To preserve electrical neutrality, an equal amount of counterion charge must accumulate at the alumina-water interface. In the presence of electrolyte ions, the counterion charge may consist of a diffuse atmosphere of counterions or a compact layer of bound counterions or a combination of both. The complete interface, including the surface and the accumulated counterions, is often called the *electrical double layer* Background theory on the electrical double layer can be found in standard reference books.[32,34–38]

C. POINTS OF ZERO CHARGE

The balance of surface charge on an aluminum oxide mineral in aqueous solution is'"

$$\sigma_H + \sigma_{is} + \sigma_{os} + \sigma_d = 0 \quad (3)$$

where σ_H is the net proton charge, defined by $\sigma_H = F(\Gamma_H - \Gamma_{OH})$, where Γ is a surface excess concentration; σ_{is} is the inner-sphere complex charge resulting from the formation of inner-sphere complexes between adsorbing ions (other than H^+ and OH-) and surface aluminol groups; σ_{os} is the outer-sphere complex charge resulting from the formation of outer-sphere complexes between adsorbing ions and surface aluminol groups or ions in inner-sphere complexes; σ_d is the dissociated charge, equal to minus the surface charge neutralized by electrolyte ions in solution that have not formed adsorbed complexes with surface aluminol groups.

Points of zero charge are pH values associated with specific requirements on surface charge.[7] The point of zero charge, p.z.c., is the solution pH value where total net particle charge is zero: $\sigma_H + \sigma_{is} + \sigma_{os} = \sigma_d = 0$.[7] The p.z.c. can be measured directly using electrokinetic measurements or colloidal stability experiments.[40] When the p.z.c. is measured using electrokinetics it is often called the isoelectric point, i.e.p.. The point of zero net proton charge, p.z.n.p.c., is the solution pH value where net proton charge, σ_H is zero.[7] The p.z.n.p.c. can be measured using potentiometric titration if only proton-selective aluminol groups are titrated. The point of zero salt effect, p.z.s.e., is the solution pH value where the net proton charge is independent of solution ionic strength: $\partial\sigma_H/\partial I = 0$.[7] The p.z.s.e. can also be measured by potentiometric titration using either batch or continuous titrations. The point of zero net charge, p.z.n.c., is the solution pH value where the difference between cation exchange capacity, CEC, and anion exchange capacity, AEC, is zero. This condition is identical to $\sigma_{os} + \sigma_d = 0$.

van Riemsdijk et al.[41] recently proposed that the p.z.c. at which no specific adsorption is indicated should be referred to as the pristine point of zero charge, or p.p.z.c., to distinguish this p.z.c. from other p.z.c. values (at which specific adsorption occurs). This appears to be an excellent nomenclature suggestion; the p.z.c. in the presence of specific adsorption represents the pH at which the surface proton balance equals zero, which may not be the pH at which there is zero surface charge. The condition of zero surface charge can only be indicated unambiguously by zero electrophoretic mobility.

1. Electrokinetic Potentials and Coagulation Rate

Electrokinetic techniques for inferring the electrical potential difference across the alumina-water interface rely on the relative movement between surface and solution. Some water is strongly bound by the alumina surface and moves along with the particles when placed in an electric field. At some distance from the surface, a shear plane develops where the water movement is independent of the particles. The shear plane is assumed generally to occur within the electrical double layer. The relative motion of the alumina with respect to the bulk solution results in a separation of charge, and a potential difference is created across the shear plane; this potential difference is referred to as the zeta potential.[32,42]

Electrophoresis measures the movement of a charged particle in response to an applied electric field, known as electrophoretic mobility. Electroosmosis measures the movement of an electrolyte solution near an interface in response to an applied electric field, known as electroosmotic velocity. The streaming potential is induced by the movement of an electrolyte solution near an interface in response to an applied pressure gradient. The sedimentation potential is induced by the gravity settling of a charged particle.[7] Table 1 provides a compilation of p.z.c. values obtained directly from electrokinetic measurements and coagulation rate studies.

Table 1 Direct Measurement of i.e.p.

Solid	i.e.p.	Electrolyte	Ref.
	Electrophoresis		
γ-Al_2O_3	8.9	KNO_3	43
γ-Al_2O_3	9.0-9.7	NaClO,	165
γ-Al_2O_3	9.5		167
γ-Al_2O_3	9.5-9.8	NaCl	205
γ-Al_2O_3	8.1	NaCl	45
δ-Al_2O_3	9.1	NaClO,	124
δ-Al_2O_3	9.2	NaClO,	108
δ-Al_2O_3	8.6	KCl	46
η-Al_2O_3	8.4	KCl	46
α-Al_2O_3	9.1	KCl	49
Al_2O_3	9.1	KNO_3	79
Gibbsite	10.0	$NaNO_3$	54
Gibbsite	9.6	NaCl	149
Boehmite	10.4	NaClO,	50
Boehmite	9.1	KNO_3	47
Boehmite	9.4	KCl	146
Pseudoboehmite	9.2	$NaNO_3$	148
$Al(OH)_3$	8.9		206
$Al(OH)_3$ gel	8.2	NaCl	48
$Al(OH)_3$ gel	8.4	NaCl	48
Amorphous $Al(OH)_3$	8.5	NaClO,	122
Amorphous $Al(OH)_3$	8.6	NaClO,	124
Amorphous $Al(OH)_3$	9.5	NaCl	207
	Streaming Potential		
γ-Al_2O_3	9.0-9.2	LiCl, KCl	44
α-Al_2O_3	9.2		208
	Coagulation Rate		
γ-Al_2O_3	8.9	KNO_3	43
α-Al_2O_3	9.0	KCl, KClO,	49
α-Al_2O_3	9.1	KNO_3	49

Additional compilations of early work are provided by Yopps and Fuerstenau[49] and Parks.[209]

Wiese and Healy[43] have studied the effect of pH and electrolyte concentration on the zeta potential of γ-Al_2O_3 colloidal particles suspended in KNO_3 solutions (Figure 8). The i.e.p., the pH value at which the zeta potential is zero, was reported as 8.9, very close to the values found in potentiometric titrations of γ-Al_2O_3 samples. At a given pH value (except the i.e.p.), the zeta potential increases in absolute value as the electrolyte concentration decreases (Figure 8). The absolute value of the zeta potential increases rapidly with pH near the i.e.p. but the slope of the curves decreases considerably at pH values far from the i.e.p. Similar behavior was found for γ-Al_2O_3 in NaCl[44,45] and KCl solutions, η-Al_2O_3 in KCl solutions,"" boehmite in KNO_3 solutions," and amorphous aluminum oxides in NaCl solutions.[48]

The decrease in zeta potential with electrolyte concentration at a given pH is in contrast to the dependence of the surface proton balance on electrolyte concentration (Figure 9). Since the zeta potential decreases in absolute value with increasing electrolyte concentration, one must conclude that either (1) a greater percentage of counterion

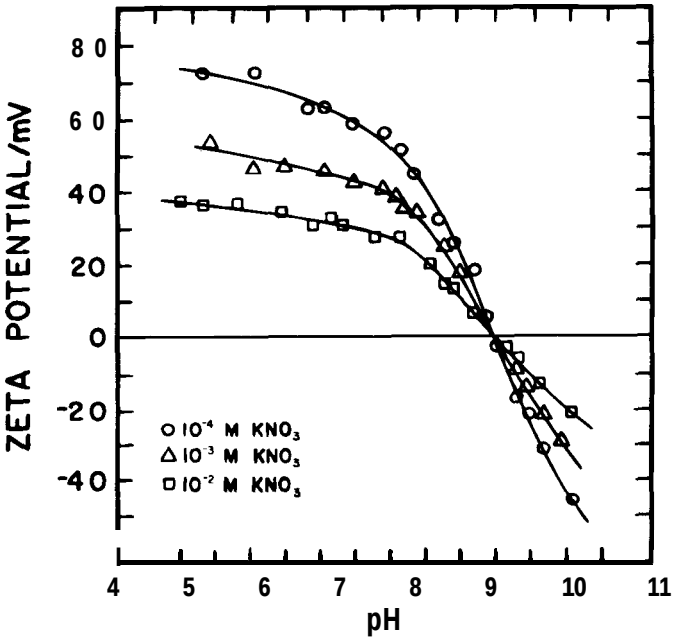

Figure 8 pH and ionic strength dependence of the zeta potential of γ-Al_2O_3. (From Wiese, G. R. and Healy, T. W., J. *Colloid Interface Sci.*, 51, 427, 1975. With permission.)

charge is present inside the hydrodynamic shear plane at higher electrolyte concentrations or (2) the location of the hydrodynamic shear plane is farther away from the alumina surface at higher electrolyte concentrations.

Yopps and Fuerstenau[49] studied the variation in zeta potential of α-Al_2O_3 as a function of pH and type of electrolyte medium. An i.e.p. of 9.1 was reported, in agreement with their titration determination for the same sample. Relatively large mobilities were observed in comparison to those measured under similar conditions for γ-Al_2O_3. Yopps and Fuerstenau[49] also compared the mobilities of α-Al_2O_3 particles suspended in 0.001 mol dm^{-3} solutions of $KClO_4$, KNO_3, and KCl. The mobilities of the particles were the same in all three electrolyte solutions when pH > i.e.p., i.e., when the particles were negatively charged. When pH < i.e.p. and the particles were positively charged, however, the mobility of the particles depended upon the anion present in the system. Tschapek et al.[44] compared the streaming potential of γ-Al_2O_3 particles in 0.001 mol dm^{-3} solutions of KCI and LiCl. The streaming potentials depended upon the cation present (except at the i.e.p.).

Bleam and McBride[50] reported an i.e.p. of 10.4 for boehmite. The data reported by these authors were unique in that little dependence of particle mobility on electrolyte concentration was observed in very dilute solutions of $NaClO_4$.

Wiese and Healy[43] studied the rate of coagulation of γ-Al_2O_3 suspensions as a function of pH, electrolyte concentration, and suspension density. The maximum rate of coagulation was observed in the pH region near the i.e.p. Rapid coagulation occurred

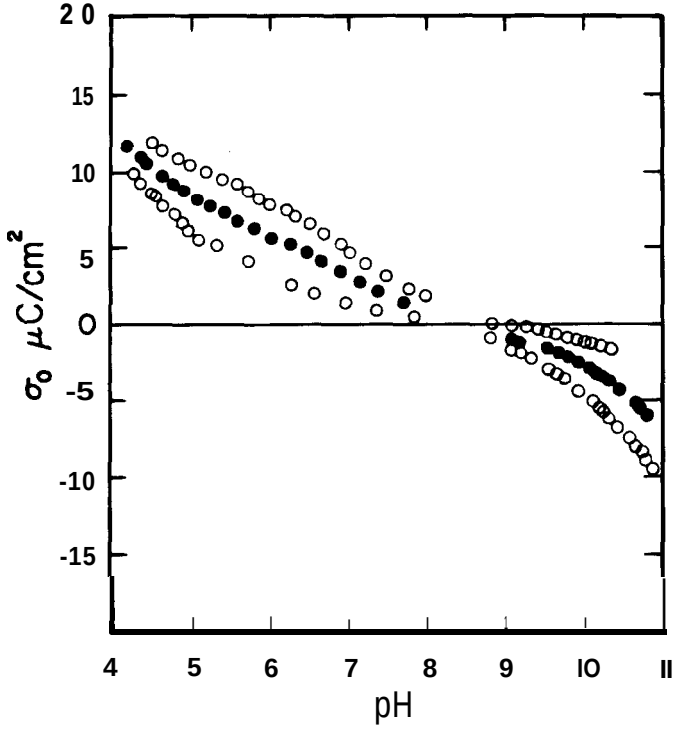

Figure 9 pH and ionic strength dependence of the net proton balance of γ-Al_2O_3. (Modified from James, R. 0. and Parks, G. A., in *Surface and ColloidScience,* Vol. 12, Matijevic, E., Ed., Plenum Press, New York, 1982, 119; data from Huang, C.-P and Stumm, W., J. *Colloid Interface Sci., 43, 409,* 1973.)

when the absolute value of the zeta potential was less than 14 mV, regardless of the pH value, electrolyte concentration, or suspension density. Yopps and Fuerstenau[49] found that the maximum coagulation rate of α-Al_2O_3 suspensions occurred in the pH region of the i.e.p. and was independent of ionic strength (Figure 10).

2. Acid-Base Potentiometric Titrations

Proton or hydroxide ion consumption by a solid phase is determined by comparing the titration curve of a suspension in an electrolyte solution with that of the electrolyte alone. Details of the methodology are given by Huang.[51] The adsorption isotherm for the proton is obtained with the mass balance equation:

$$A\Gamma = (C_A - C_B) - (C_H - C_{OH}) \quad (4)$$

where $\Gamma = (\Gamma_H - \Gamma_{OH})$ is the net surface excess of hydrogen over hydroxide ions per square centimeter of surface, A is the total surface area of the solid per unit volume (cm^2/dm^3), C_A and C_B the concentrations of acid and base added to reach a given point

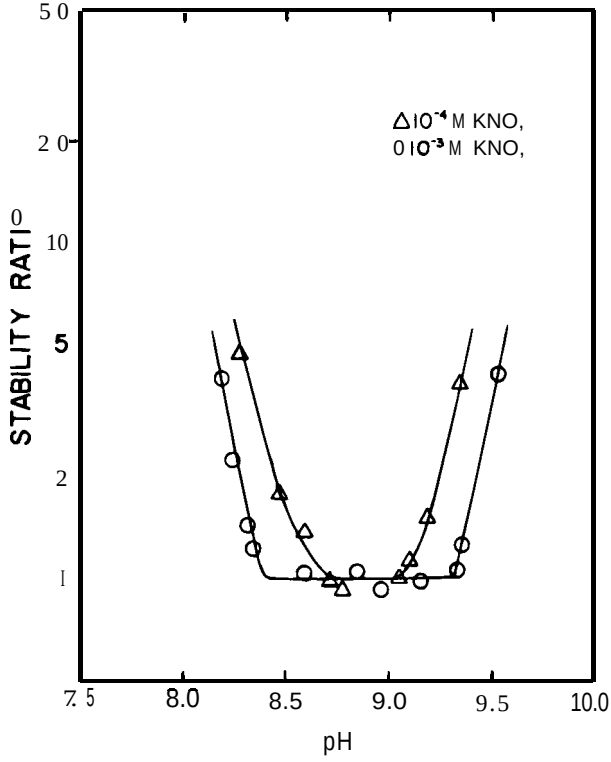

Figure 10 pH and ionic strength dependence of the coagulation rate of γ-Al_2O_3. (Modified from Wiese, G. R. and Healy, T. W., J. Colloid *Interface Sci.,* 51, 427, 1975.)

in the titration curve, and C_H and C_{OH} are the concentrations of hydrogen and hydroxide ions, respectively. If the supporting electrolyte ions have no specific affinity for the surface, or if the positive and negative ions of the supporting electrolyte have equal specific affinity, then curves representing Γ as a function of pH for each of several electrolyte concentrations should intersect at a common pH value, the p.z.c.,[52] where:

$$\Gamma_H - \Gamma_{OH} = 0 \tag{5}$$

Figure 10 shows plots of Γ as a function of pH and sodium chloride concentration for titrations of γ-Al_2O_3.[53] The intersection point indicates a p.z.c. of 8.5. Note that the protons released or consumed by the alumina increase with electrolyte concentration. The surface is positively charged at pH values below 8.5 and negatively charged when the pH is greater than 8.5. Table 2 provides a compilation of p.z.c. values obtained from potentiometric titrations.

Kavanagh et al.[54] studied the proton balance in potentiometric titrations of gibbsite as a function of pH and $NaNO_3$ concentration (0.01 to 1 mol dm^{-3}). The data are somewhat unique in comparison to γ-Al_2O_3 and other oxides, in that the quantity Γ is less sensitive to electrolyte concentration. The authors reported a p.z.c. value of 9.8 for

Table 2 Potentiometric Titration Measurements

Solid	p.z.s.e.	Electrolyte	Ref.
γ-Al_2O_3	a.5	NaCl	53
γ-Al_2O_3	a.6	LiCl	44
γ-Al_2O_3	9.1	KCl	44
γ-Al_2O_3	8.8	NaBr	67
γ-Al_2O_3	5.4	KNO_3	56
γ-Al_2O_3	7.0	NaClO,	144
γ-Al_2O_3	8.1	NaCl	45
δ-Al_2O_3	a.5	KCl	46
η-Al_2O_3	a.5	KCl	46
α-Al_2O_3	9.1	KCl	49
α-Al_2O_3	4.8	KNO,	57
Al_2O_3	a.9	KCl	210
Al_2O_3	9.1	KNO_3	55
Al_2O_3	7.2	$NaNO_3$	211
Gibbsite	7.8	NaCl	63
Gibbsite	9.5	NaCl	63
Gibbsite	9.8	$NaNO_3$	54
Boehmite	8.5	KNO_3	47
Boehmite	7.2	KCl	146
$Al(OH)_3$	8.2	NaCl	48
$Al(OH)_3$	8.4	NaCl	48
$Al(OH)_3$ gel	9.7		212
$Al(OH)_3$ gel	9.7	KCl	213
Amorphous $Al(OH)_3$	9.5		97
	p.z.n.p.c.		
γ-Al_2O_3	8.3	$NaClO_4$	90
γ-Al_2O_3	8.7	$NaClO_4$	12
Pseudoboehmite	9.3	$NaClO_4$	214

Additional compilations of early work are provided by Yopps and Fuerstenau[49] and Parks.[209]

gibbsite. Titration data for Al_2O_3 as a function of pH and electrolyte concentration were published by Tewari and McLean.[55] These authors found that p.z.c. decreased with increasing temperature from a value of 9.1 at 30°C to 8.4 at 90°C. The change in p.z.c. with temperature appeared to be explained solely by the change in the ionization constant of water as a function of temperature. In contrast, Akratopulu et al.[56] found that p.z.c. of γ-Al_2O_3 increased with increasing temperature from a value of 4.5 at 10°C to 9.0 at 50°C.

Smit and Holten[17] and Ahmed[57] have reported p.z.c. values for α-Al_2O_3 of 4.5 and 4.8; the former investigators studied a large crystal while the latter author worked with a powder. The lower p.z.c. of α-Al_2O_3 can be expected on the basis of crystal structure. The dehydrated oxide has hydroxyl groups which are more polarized than those in the aluminum hydroxides, because of differences in the coordination number of the aluminum ion. This difference will result in a relatively acidic surface for the oxide and a more basic surface for $Al(OH)_3$.[58]

In contrast, Yopps and Fuerstenau[49] observed a p.z.c. of 9.1 in studies of an alumina identified as α-Al_2O_3 by X-ray diffraction. The authors also cite several other publications that have found the value of p.z.c. to fall in this range. However, Smit and Holten[17] state that grinding α-Al_2O_3 results in a disturbed surface layer which, upon contact with

water, hydrates to give a surface layer like that of gibbsite. This could result in artificially high values of p.z.c. for α-Al_2O_3 powders. A study by Smith"' found that α-Al_2O_3 had a p.z.c. of 9.0 to 9.1 after 3 d of immersion in water, but after 3 months the p.z.c. had risen to pH 10.1 to 10.2. These results suggest that the α-Al_2O_3 surface may undergo alteration in water to give an external "shell" of gibbsite. Support for this hypothesis was given by electron micrographs of altered α-Al_2O_3 particles, which showed the presence of hexagonal microcrystals of gibbsite on the particle surfaces.[59] Slow alteration of the surfaces of other aluminum oxides and hydroxides may also occur, since gibbsite is probably the thermodynamically stable phase at 25°C.[19,60] The surfaces of gibbsite preparations may also vary in their degree of crystallinity, which may influence their solubility, surface area, concentration of structural defects, and rates of recrystallization.[61]

The increase in positive charge (as indicated by the increase in p.z.c.) can be attributed to localized strong positive charge on the edges of gibbsite crystals, as compared to the more diffuse distribution of surface charge expected for the dehydrated material. The distribution of charge sites per unit area of crystal faces of well-crystallized gibbsite, however, would be expected to be sparse. As noted previously, bayerite crystals grow preferentially in the *c* direction and therefore a substantial fraction of the surface of an individual bayerite crystal comprises the edges of individual layers, not the faces.

The relative acidity of oxide surfaces can be inferred from values of the p.z.c. and, therefore, alumina is usually less acidic than silica or titania.[51] A quantitative evaluation of the acidity of aluminol groups on a surface, however, requires a model for the surface reactions and the introduction of several assumptions. Models that have been used to describe the surface reactions will be discussed below. The quantity, Γ, the net proton adsorption density defined in Equation 5, is usually called "surface charge" in the literature. It is important to remember that the experimental quantity determined is the net proton release or consumption of the surface, which is not an actual determination of surface charge. If not properly taken into account,.[51,62] the dissolution of alumina during titrations may significantly affect the titration curve and hence the net surface proton balance, Γ.

3. *Measurement of Counterion Adsorption*

Ionic composition of counterion charge was studied directly on gibbsite,[63,64] δ-Al_2O_3, and η-Al_2O_3.[46] These measurements of the pH dependence of counterion adsorption and others made by Breeuwsma and Lyklema[65] on hematite led to the general conclusion that many univalent ions (e.g., Na^+, Cl^-) were not specifically adsorbed but were held at the surface only by electrostatic forces just to balance the surface charge. Figure 11 shows plots of counterion adsorption of potassium chloride as a function of pH on two aluminas.

Recently, several experimental studies[17,66,67] have reopened the subject of counterion binding by oxide surfaces. Sprycha[67] found that the net charge from adsorption of Na^+ and Br^- ions on γ-Al_2O_3 was greater than the surface proton balance in the pH region near the p.z.c.. At the p.z.c., adsorption of Na^+ was nearly equal to adsorption of Br^-, but both quantities were significantly greater than the surface proton balance. Adsorption of Na^+ was significant at pH < p.z.c. (when the surface was positively charged) as was adsorption of Br^- at pH > p.z.c.. Supporting evidence for this behavior can be found in studies of γ-Al_2O_3 suspended in NaBr solutions,[68] of α-Al_2O_3 crystals suspended in

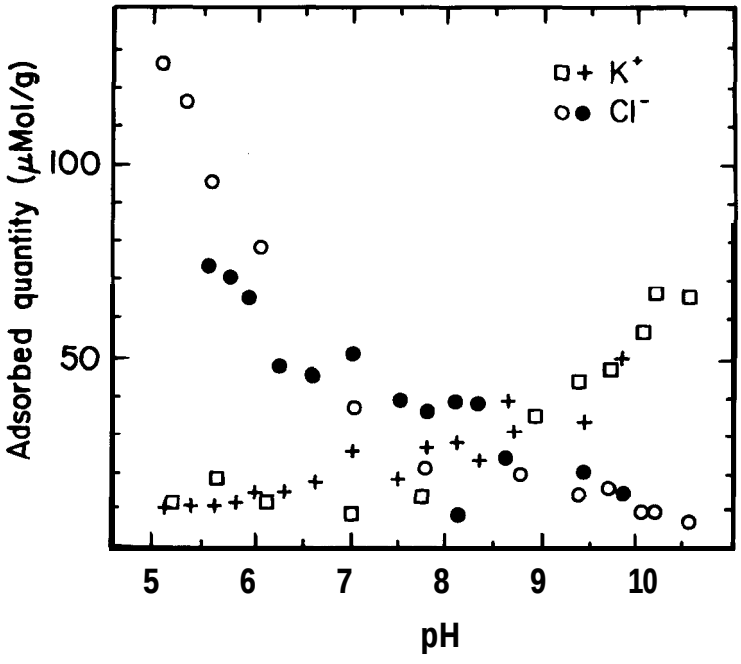

Figure 11 pH dependence of counterion adsorption on δ-Al_2O_3 (closed symbols) and η-Al_2O_3 (open symbols). (From Thomas, F., Bottero, J. Y, and Cases, J. M., *Colloids Surf.,* 37, 281, 1989. With permission.)

NaBr solution," and of colloidal samples of titanium dioxide suspended in uni-univalent electrolyte solutions.'"

Yates et al.[70] suggested that counterions form weak ion pairs with charged surface hydroxyl groups, and this may explain the observations of specifically adsorbed counterions at the p.z.c. Ion pair formation at alumina surfaces in NaBr solutions could be described by electrolyte binding reactions, i.e.,

$$AlO^- + Na^+ = AlO^-Na^+ \quad (6)$$

$$AlOH_2^+ + Br^- = AlOH_2^+Br^- \quad (7)$$

Equation 7 refers to ion pair formation with a Bronsted acid site, $AlOH_2^+$, but it is also possible that the reaction proceeds by complex formation at a Lewis acid site (by ligand exchange) as postulated by Smit and Holten,[17] i.e.,

$$AlOH_2^+ + Br^- = Al^+Br^- + H_2O \quad (8)$$

The formation of ion pairs with charged aluminol groups may explain other experimental observations: (1) the dependence of surface proton balance and electrokinetic potential on electrolyte concentration'* and (2) the failure of the Nernst equation to describe the pH dependence of the surface potential," as will be described in Section III.D.

Smit and Holten[17] found an i.e.p. near pH 3.5 for single crystals of α-Al_2O_3 in NaBr solutions; a p.z.c. of 4.5 from counterion adsorption was reported for the same samples. The low value for i.e.p. in comparison to published values for powdered samples was attributed to sample grinding. The fact that the i.e.p. was lower than the p.z.c. from counterion adsorption was evidence for specific adsorption of bromide ions. The authors studied the binding of sodium and bromide ions on the crystal surface and found that both ions were indeed specifically adsorbed.

Equality between the p.z.c., p.z.n.c., and the p.z.s.e. is expected if the aluminum oxide is suspended in a 1:1 background electrolyte that forms only outer-sphere surface complexes. If the oxide is suspended in a 1: 1 background electrolyte along with a fixed concentration of a specifically adsorbing ion, the p.z.c. and the p.z.s.e. are still expected to be equal but shift above/below the p.z.c. without specific adsorption for specific cation/anion adsorption. If the oxide is suspended in a specifically adsorbing background electrolyte, p.z.c. is not expected to equal p.z.s.e. and p.z.s.e. is shifted below/above the p.z.c. without specific adsorption for specific cation/anion adsorption.^7

D. MEASUREMENT OF SURFACE POTENTIAL

The measurement of changes in electrical surface potential between an insulating material, e.g., alumina, and an aqueous solution can be made by incorporating a thin film of alumina in an electrolyte/alumina/silicon structure.[71] A field effect transistor (ISFET device) then can be fabricated to measure lateral current flow, and relative changes in the surface potential of alumina can be measured.[72,73]

Potential-determining ions (pdi), by definition, are ions that determine the interfacial electrical potential difference by virtue of their equilibrium distribution between solid and liquid phases.[74] The half-cell potentials of reversible electrodes, such as AgI, are established by transfer of charge in the form of pdi between the two bulk phases.[32] In the case of AgI, the pdi are Ag^+ and II, and the potential difference between the two phases is given by the Nernst equation,

$$E = E^0 + RT/F[\ln\{Ag^+\} - \ln\{Ag^+\}^0] \quad (9)$$

where E^0 is a reference potential and $\{Ag^+\}^0$ is the silver ion concentration at that reference potential. Many of the early research studies of oxide-water interfaces assumed that hydrogen and hydroxide ions were pdi. For example, for the solid Al_2O_3, it could be argued that Al^{3+} and O^{2-} are the pdi, e.g., where ψ_o is the surface potential. Since the activities of both Al^{3+} and O^{2-} may be small and highly pH dependent in most solutions, the Nernst equation can be written more conveniently in terms of pH.

$$\psi_o = 2.3\ RT/3F[\log\{Al^{3+}\} - \log\{Al^{3+}\}_{p.z.c.}] \quad (10)$$

$\{Al^{3+}\}$ is related directly to $\{H^+\}$ through the solubility product constant for alumina and, thus, Equation 10 maybe rewritten in terms of H^+:

$$\psi_o = 2.3\ RT/F(p.z.c. - pH) \quad (11)$$

In this way, H^+ and OH^- may be considered as pdi and, according to the Nernst equation, ψ_o will change 59.2 mV per pH unit at 25°C.

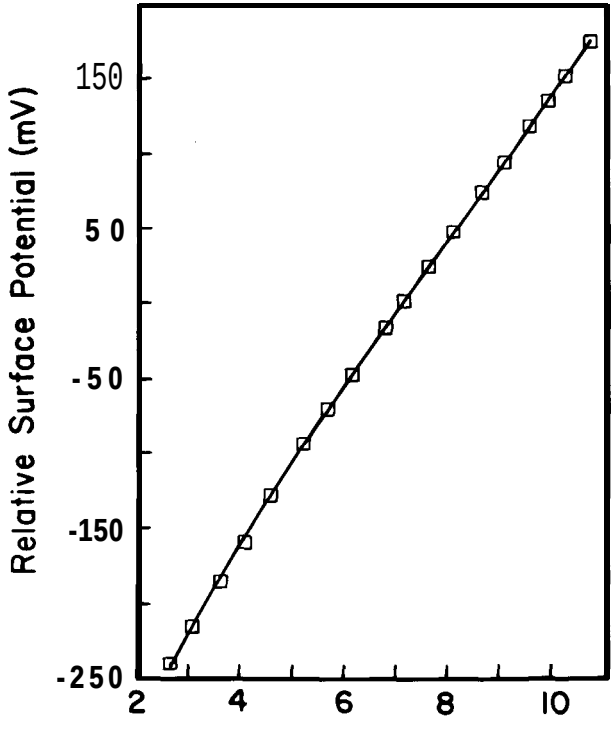

Figure 12 pH dependence of the surface potential Ψ_o, of γ-Al_2O_3 in 0.1 mol dm ^{3} $NaNO_3$ solution. (From Bousse, L., de Rooij, N. F., and Bergveld, P., IEEE Trans., Elect. Devices, 30, 1263, 1983. With permission.)

Bousse et al.^73 measured the pH dependence of the surface potential of γ-Al_2O_3 in 0.1 mol dm^{-3} $NaNO_3$ with an ISFET device (Figure 12). The dependence of ψ_o on pH was not consistent with the Nernst equation, in that the slope was less than 59.2 mV per pH unit and the relationship was not quite linear.[71] The smallest slope (48 mV per pH) was measured near the p.z.c. (pH 8.0). At pH values less than the p.z.c., the slope increased to about 56 mV per pH unit; above the p.z.c., the slope increased to values as high as 53 mV. The failure of the Nernst equation to describe the surface potential relationship is an indication that counterions form complexes (or ion pairs) with charged aluminol groups on the surface.^71

IV. ADSORPTION OF METAL IONS

Numerous studies of the adsorption of metal ions on aluminum oxides and hydroxides have been conducted. It has been demonstrated often that the mechanism of metal ion association with hydrous oxide surfaces involves an ion exchange process in which the adsorbed metal ions replace bound protons.[53,75–77] The adsorption of metal ions from dilute solution onto alumina surfaces is highly dependent-on pH, as has been demonstrated

by several investigators (Table 3). Figure 13 illustrates data of Benjamin and Leckie[78] for Cd^{2+} adsorption on γ-Al_2O_3. These authors were among the first to demonstrate that the pH region in which adsorption increases rapidly (the "adsorption edge") depends on metal concentration. This is true even at very low concentrations of metals, far below those that would saturate the maximum adsorption capacity of γ-Al_2O_3. A consequence of this phenomenon is that adsorption isotherms for metal ions on aluminas usually are well described by the Freundlich equation:

$$\Gamma_M = aC_M^b \tag{12}$$

where Γ_M is the adsorption density of the metal ion, C_M is the equilibrium concentration of the metal ion, and a and b are empirical constants. The parameter b usually has a value in the range of 0.5 to 0.7 for metal ion adsorption on alumina. A maximum in adsorption density for metal ions is often not evaluated because of experimental difficulties. Spectroscopic studies generally have led to the conclusion that there is a continuum of adsorption phenomena from monolayer adsorption to cluster formation or multilayer adsorption and, finally, surface precipitation.[10,50,79–81]

At very low concentrations, the adsorption of metal ions can be considered as a bimolecular adsorption/desorption reaction in which a metal ion is bound by an aluminol group, releasing a proton to solution, i.e.,

$$AlOH + Pb^{2+} = AlOPb^{+} + H^{+} \tag{13}$$

Hachiya et al.[82–84] and Yasunaga and Ikeda[85] have shown by electric field pulse and pressure-jump methods that the adsorption and desorption reactions are very fast, with half-times considerably less than 1 s under typical experimental conditions. However, additional slow uptake of metal ions is often observed over hours or days (e.g., Cd^{2+} adsorption on γ-Al_2O_3,[86] Cr^{3+} and VO^{2+} adsorption on δ-Al_2O_3,[87] and Cu^{2+} adsorption on amorphous aluminum hydroxide*"). The slow processes are very poorly understood. If the γ-Al_2O_3 surface has been altered to form a gibbsite-like layer, perhaps the slower process could be caused by diffusion through or around reorganized surface material to deeper layers.

As metal ions are adsorbed, protons are released (Equation 13). Most of these protons are readsorbed by the surface through ion-pair formation or the protonation of aluminol groups, but some remain in solution. The protons released during metal adsorption can be determined by back titration to constant pH[88,89] or by measuring the displacement of potentiometric titration curves.[53,90] The number of H^+ ions released per metal ion adsorbed is usually found to have a noninteger value between 1 and 2.[91] For example, Hohl and Stumm[90] found an average value of 1.5 protons released per Pb^{2+} ion adsorbed on γ-Al_2O_3. Because the overall proton release usually shows values much greater than one, many authors[77,88–90,92] have assumed that a second adsorption reaction must be considered in which two protons are released per metal ion adsorbed, e.g.,

$$AlOH + Pb^{2+} + H_2O = AlOPbOH + 2H^{+} \tag{14}$$

$$2AlOH + Pb^{2+} = \begin{matrix} AlO\backslash \\ AlO/ \end{matrix} Pb + 2H^{+} \tag{15}$$

Table 3 Adsorption of Metal Ions

Solid	Cations	Study type*	Ref.
γ-Al_2O_3	Ca, Mg, Sr, Ba	a, b, e, f	53
γ-Al_2O_3	Pb	a, f	90
γ-Al_2O_3	Pb	b, c	82
γ-Al_2O_3	Cd, Cu, Zn, Pb	a, b, j, k	86
γ-Al_2O_3	cu	b, k	105
γ-Al_2O_3	Pb, Cu	a, j	78
γ-Al_2O_3	Co, Cd, Cs, Sr, Eu	a, b, i	103
γ-Al_2O_3	Cd	a, k	215
γ-Al_2O_3	Cu, Zn	h, k	101
γ-Al_2O_3	Cu, Cd	a, k	116
γ-Al_2O_3	Cu, Mn, Zn, Co, Pb	a, b, c, e	83, 84
γ-Al_2O_3	Cu, Mn, Zn, Co, Pb	a, c, e	85
γ-Al_2O_3	Ni, Ca, Cd, Cu, Pb, Zn	a, e, g, k	106
γ-Al_2O_3	Ni. Zn. Pb	a, k	107
γ-Al_2O_3	Pb	a, d	98
γ-Al_2O_3	Co, Ni	a, b, e, f	100
δ-Al_2O_3	cu	d	93
δ-Al_2O_3	Ni	a	216
δ-Al_2O_3	Cr, V	a, c	87
δ-Al_2O_3	cu	d, k	94
δ-Al_2O_3	Cr	a, d	99
δ-Al_2O_3	co	a, k	108
α-Al_2O_3	Zn	a	217
α-Al_2O_3	Cd	a, b, f, h	102
α-Al_2O_3	Cd	a, b, f, h	91
α-Al_2O_3	Cd	a, b, k	115
Gibbsite	Ca	d	145
Gibbsite	Ca	d	218
Gibbsite	cu	a, b, c, d	80
Gibbsite	cu	a, d	10
Gibbsite	Cu, Zn, Mg	a	219
Boehmite	cu	a, b, c, d	80
Boehmite	Mn, Mg	a, d, e	50
$Al(OH)_3$	Cu, Co, Zn, Ni, Pb, Cd	a	220
$Al(OH)_3$	Cd, Zn	a	206, 221
$Al(OH)_3$ gel	Ca, Sr	a,h	222
$Al(OH)_3$ gel	Cu, Pb, Ni, Zn, Co, Cd, Mg, Ca, Sr, Ba	a,j	223
$Al(OH)_3$ gel	Zn, Cd	a	224
$Al(OH)_3$ gel	cu	b, d	225
$Al(OH)_3$ gel	cu, v	b, d, k	96
$Al(OH)_3$ gel	cu	b, d, k	81
Hydrous Al_2O_3	Cu, Zn, Mg	a	219
Amorphous $Al(OH)_3$	cu	a, b, c, d	80
Amorphous $Al(OH)_3$	Mn	d	97
Amorphous $Al(OH)_3$	Zn	a, k	104
Amorphous $Al(OH)_3$	cu	a, d, k	109
Amorphous $Al(OH)_3$	cu	a, d, k	111
Amorphous $Al(OH)_3$	cu	a, d, k	113
Amorphous $Al(OH)_3$	cu	a, d, k	112
Amorphous $Al(OH)_3$	cu	a, d, k	114
Amorphous $Al(OH)_3$	V	a, d, k	110

* a, dependence on pH; b, dependence on metal concentration; c, kinetics; d, spectroscopy; e, electrokinetics; f, proton release; g, dependence on temperature; h, dependence on suspension density; i, dependence on ionic strength; j, dependence on competing metal concentration; k, dependence on competing or complexing ligand concentration.

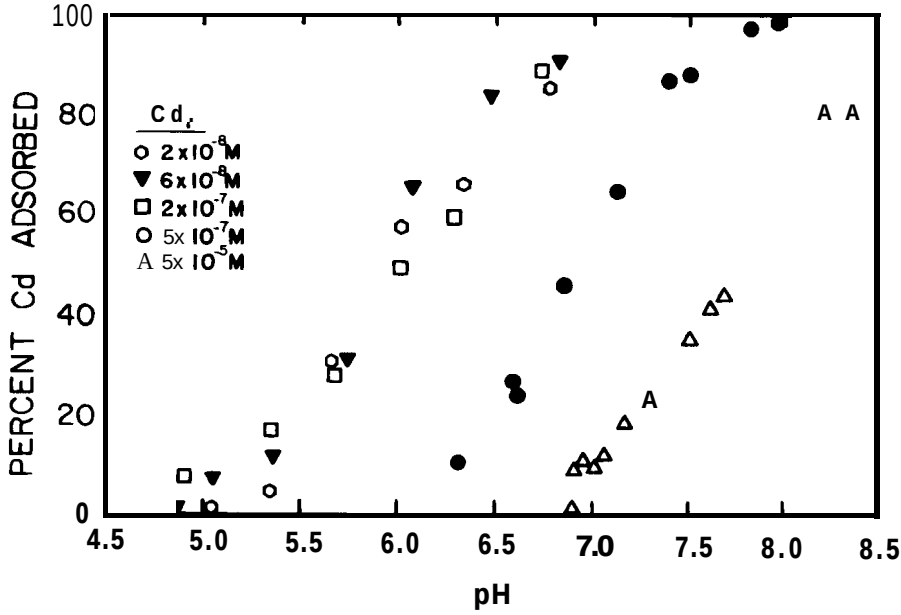

Figure 13 Adsorption of Cd^{2+} on γ-Al_2O_3 from 0.1 mol dm^{-3} $NaNO_3$ solution as a function of pH and metal concentration. (From Benjamin, M. M. and Leckie, J. O., in Contaminants and Sediments, Vol. 2, Baker, R. A., Ed., Ann Arbor Science, Ann Arbor, MI, 1980, 305. With permission.)

The fractional and nonequivalent values observed for the stoichiometry result from the fact that the equilibria of ion-pair and surface ionization reactions (Equations 1, 2, 6, and 7) are perturbed by the adsorption of metal ions. Few authors have taken these reactions into account when evaluating the stoichiometry of metal adsorption from dilute solution.[89,91] Hohl and Stumm[90] concluded that the bidentate complexation of Pb^{2+} (Equation 15) was insignificant in comparison to monodentate complexes formed on the γ-Al_2O_3 surface.

On the other hand, spectroscopic studies have typically found that the alumina surface acts as a bidentate ligand in binding Cu^{2+} (Figure 14).[10,80,93,94] Rudin and Motschi[93] found from a combination of EPR (electron paramagnetic resonance) and ENDOR (electron nuclear double resonance) spectra that Cu^{2+} formed inner-sphere surface complexes of predominantly pseudo-square planar geometry. The conclusion that a bidentate complex was formed was based on an interrelation between the surface stability constant and the values of EPR parameters'" and a comparison of these parameters to those of aqueous Cu(II) complexes.'" Motschi and Rudin[95] also suggested a bidentate inner-sphere surface complex for VO^{2+} adsorption on δ-Al_2O_3 from ENDOR results. Using a combination of ENDOR and ESEEM (electron spin echo envelope modulation) spectroscopic data, Möhl et al.[94] also suggested the formation of inner-sphere bidentate Cu^{2+} complexes on δ-Al_2O_3. Ligands containing nitrogen groups formed ternary complexes at the surface by coordination of Cu^{2+} in the equatorial positions

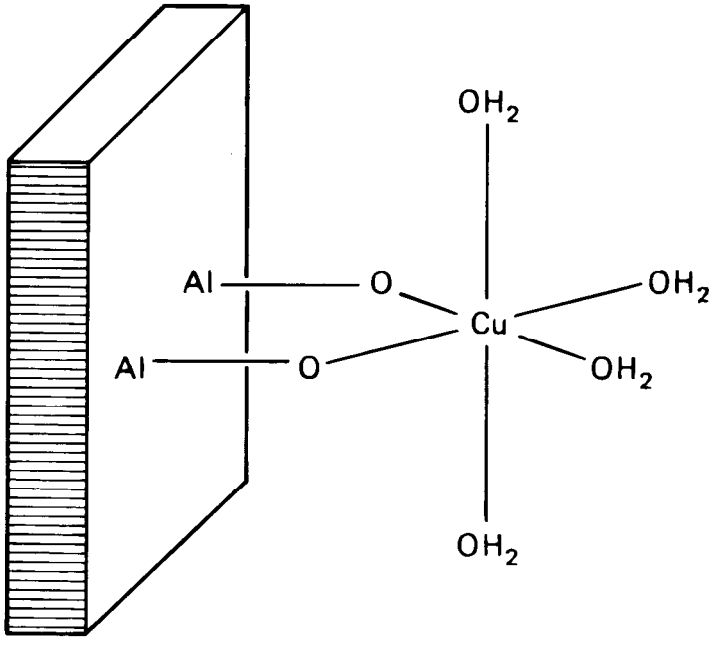

Figure 14 Suggested structure of the coordinative complex formed by Cu^{2+} with two aluminol groups of the γ-Al_2O_3 surface. (Modified from Rudin, M. and Motschi, H., J. *Colloid Interface Sci., 98,* 285, 1984.)

instead of the axial positions.“” Chemisorption was found to be the adsorption mechanism for Cu^{2+} and VO^{2+} on amorphous aluminum hydroxide using ESR spectroscopy.^96 Manganese, on the other hand, was adsorbed as a hydrated outer-sphere complex on aluminum hydroxide, as observed with ESR spectroscopy.^97

Chisholm-Brause et al.[98] studied Pb^{2+} adsorption on γ-Al_2O_3 using a combination of XANES (X-ray absorption near edge structure) and EXAFS (extended X-ray absorption fine structure) spectroscopies and concluded that inner-sphere, predominantly monodentate complexes were formed. Karthein et al.[99] observed Cr(III) adsorption on δ-Al_2O_3 using both ESR and ESEEM spectroscopies and found a conversion from inner-sphere to outer-sphere surface complexes over time. These authors proposed a bidentate adsorption mechanism.

A few studies have examined the effect of metal ion adsorption on the electrokinetic potential of alumina particles.[53,84,100] Huang and Stumm[53] have shown that the adsorption of Ca^{2+} increases the zeta potential of γ-Al_2O_3, increasing the i.e.p. from 9.0 in NaCl solution to near 10.5 in 0.0001 mol dm^{-3} $CaCl_2$. At some pH values (e.g., pH 9.5), a reversal of charge was demonstrated upon adsorption of Ca^{2+}. The γ-Al_2O_3 particles were negatively charged at low concentrations of Ca^{2+}, but became positively charged as the concentration of Ca^{2+} was increased. Bleam and McBride’” observed little effect on electrophoretic mobility of boehmite from adsorption of Mn^{2+} and Mg^{2+} and concluded that adsorption of these ions occurred via surface cluster formation.

McBride[80] conducted one of the few studies that compared the adsorption behavior of different crystal forms of aluminum oxyhydroxides. He concluded that the strong

adsorption sites for Cu^{2+} were surface hydroxyl groups coordinated to a single aluminum ion. The Cu^{2+} sorption capacities followed the order: noncrystalline alumina > boehmite > gibbsite, which is consistent with the relative number of singly coordinated hydroxyl groups on each surface. In the simplest interpretation of the gibbsite surface, the basal planes are unreactive and the adsorption sites of cations (and anions) occur only on the edges of crystals. However, in subsequent work, McBride et al.^10 showed by electron microscopy that many gibbsite plates have crystal steps at regular intervals. Strong adsorption sites are expected to be found at edge sites that occur at these step dislocations on the basal planes. These crystal steps could also act as the nucleation sites for precipitation of $Cu(OH)_2$.[10]

Metal adsorption is also a function of the suspension density of the adsorbent.^101 For a given total metal concentration, the adsorption edge shifts to lower pH value with increasing suspension density.[91,102] Adsorption of Cs^+, Sr^{2+}, Eu^{3+}, and Cd^{2+} on Al_2O_3 decreased with increasing ionic strength of a NaCl background electrolyte, while Co^{2+} adsorption exhibited no ionic strength dependence.^103

Benjamin[86] and Benjamin and Leckie[78] have found evidence for site heterogeneity on γ-Al_2O_3 by studying the effect of the presence of Cu, Pb, and Zn on Cd adsorption. These authors postulated limited groups of sites having high selectivity for specific metal ions. Zinc and Cd compete for the same group of binding sites, whereas Cu and Pb bind preferentially to other groups of sites.

Metal adsorption on aluminum oxides is affected by the presence of inorganic ligands. Enhanced adsorption has been observed for Cd^{2+} on γ-Al_2O_3 in the presence of thiosulfate[78,86] and for Cu^{2+}, VO^{2+},[96] and Zn^{2+} on amorphous aluminum hydroxide in the presence of sulfate.[104] The increased negative charge brought to the surface by sulfate is considered to promote additional metal adsorption.[96,104] High levels of phosphate sorption on amorphous aluminum hydroxide suppressed Cu^{2+} adsorption, likely due to blocking of surface sites.[81] The presence of chloride and sulfate decreased Cd^{2+} adsorption on γ-Al_2O_3.[78,86] These authors postulated that $CdCl_x$ and $Cd(SO_4)_x$ complexes adsorb in a metal-like fashion while $Cd(S_2O_3)_x$ complexes adsorb in a ligand-like fashion.

In systems containing organic ligands metal adsorption is often enhanced at low pH and depressed at high pH by the adsorption of the metal-ligand complexes. This effect has been found for adsorption of Cu^{2+} in the presence of nitrilotriacetic acid (NTA) and aspartic acid,[105] adsorption of Ni^{2+}, Zn^{2+},[106,107] and Co^{2+} in the presence of ethylene diamine tetraacetate (EDTA),[108] and adsorption of Pb^{2+} in the presence of tiron.[107] Micera and co-workers[109–111] have observed that Cu^{2+} adsorption on amorphous aluminium hydroxide shows the above effect for some organic ligands, while other organic ligands depress Cu^{2+} adsorption at all pH values.[112–114] Fulvic acid also enhanced Cd^{2+} adsorption on α-Al_2O_3 at low pH and reduced it at high pH,[115] as did dissolved natural organic matter for Cd^{2+} and Cu^{2+} adsorption on γ-Al_2O_3.[116] However, Baccini et al.^101 found that the presence of natural organic matter depressed Cu^{2+} and Zn^{2+} adsorption on γ-Al_2O_3.

V. ADSORPTION OF INORGANIC ANIONS

Anions can adsorb on the surface of aluminum oxides by ion-pair formation with positively charged surface sites (Equation 7) or by ligand exchange with surface hydroxyls,[63,117–121] e.g.,

$$\text{AlOH} + \text{H}_2\text{PO}_4^- = \text{AlH}_2\text{PO}_4 + \text{OH}^- \quad (16)$$

$$2\text{AlOH} + \text{H}_2\text{PO}_4^- = \begin{matrix}\text{Al}\\ \text{Al}\end{matrix}\!\!\diagdown\!\!\diagup\text{HPO}_4 + \text{H}_2\text{O} + \text{OH}^- \quad (17)$$

Because these reactions are ligand-exchange reactions which replace hydroxyls on the surface, the adsorption of anions usually increases with decreasing pH.[63,102,118,122–126] Figure 15 shows the adsorption of arsenate on amorphous aluminum hydroxide as a function of pH and initial anion concentration. Adsorption of AsO_4^{3-} is greatest at low pH and decreases gradually over several pH units to zero adsorption. Adsorption of weakly bound ions is also significantly affected by the concentration of the background

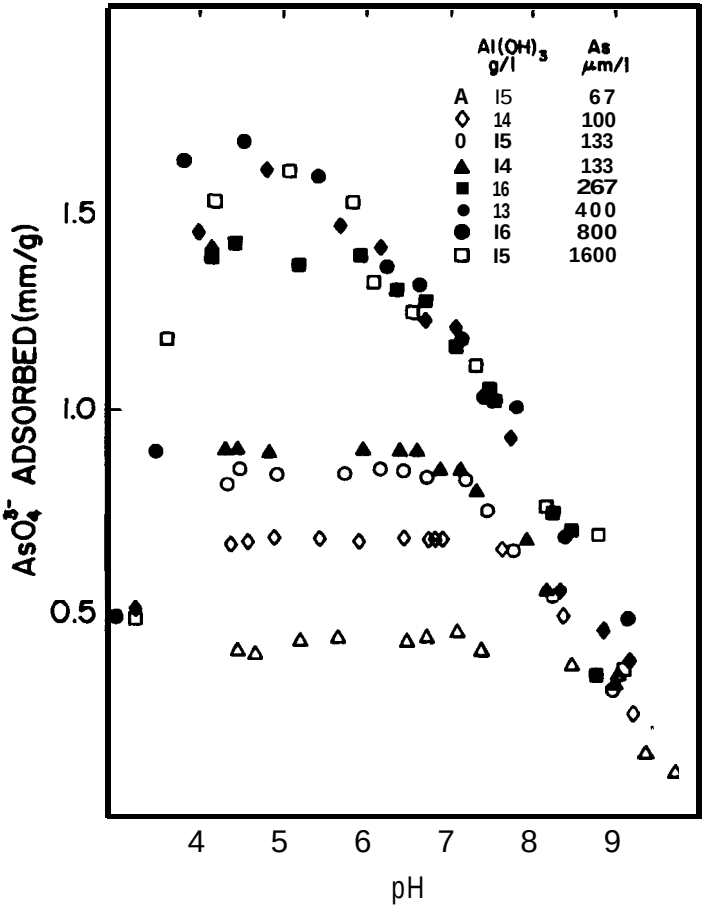

Figure 15 Adsorption of AsO_4^{3-} on amorphous $Al(OH)_3$ from 0.01 mol dm^{-3} $NaClO_4$ solution as a function of pH and anion concentration. (From Anderson, M. A., Ferguson, J. F., and Gavis, J., J. *Colloid Interface Sci.,* 53, 391, 1976. With permission.)

electrolyte.'*' The adsorption of anions that are more strongly bound (e.g., AsO_4^{3-}, PO_4^{3-}, SeO_3^{2-}) is less dependent on the ionic strength.[63,127] It is difficult to derive meaningful parameters for anion adsorption isotherms because of the slow approach to equilibrium and multiple processes occurring at the surface (see below). Nonetheless, many authors have attempted to analyze anion sorption data for a specified reaction time.[119,122,128–130] Typically a portion of the experimental data can be approximated by the Langmuir isotherm, and parameters such as the "energy of adsorption" and the "maximum adsorption capacity" are derived from these data. However, the maximum adsorption derived with one set of data frequently underestimates the actual adsorption densities measured at high adsorbate concentrations, or even may exceed an independent estimate of total adsorption sites." The studies of anion adsorption on aluminum oxides and hydroxides are numerous (Table 4). Many aspects of anion adsorption behavior have been examined, and it is difficult to make comparisons among these studies because of differences in adsorbent, kinetics of adsorption, and experimental procedures.

Because of its importance as a nutrient, phosphate has been the subject of intense study. Yasunaga and Ikeda[85] and Mikami et al.[125,126] showed that adsorption-desorption reactions of phosphate on γ-Al_2O_3 approach equilibrium rapidly. However, as was the case in cation adsorption, additional slow processes perturb the adsorption equilibria and reveal additional phosphate uptake in long-term kinetic studies.[120,129,131,132] In general, the slow processes are poorly understood. Chen et al.[131] and van Riemsdijk et al.[133] attributed the slow uptake of phosphate on α-Al_2O_3 to the formation of a surface precipitate of aluminum phosphate. An aluminum phosphate phase was found coating gibbsite particles following phosphate adsorption.[134] Phosphate desorption (and isotopic exchange) from the gibbsite surface is slow and incomplete;[118,120,129,135] this effect has been explained in terms of the high activation energy for dissociation of the binuclear-bidentate surface complex of phosphate with two aluminol groups (Equation 17) or in terms of surface precipitation of an aluminum phosphate phase at high phosphate concentrations.[135]

Nonequilibrium behavior is very evident in the studies of phosphate sorption by noncrystalline aluminum hydroxide.[136,137] Phosphate sorption and reversibility is influenced significantly by the age of the precipitate and the experimental procedures used. Phosphate uptake continues to increase even after 1 month of reaction.[133] Large differences in phosphate sorption were observed in comparing phosphate uptake on freshly precipitated aluminum hydroxide to the phosphate content of an aluminum precipitate formed in a phosphate solution.[136] The latter precipitate was reported to contain equimolar amounts of phosphorus and aluminum when formed at pH 7. If $AlPO_4$ is more stable than $Al(OH)_3$ under these conditions,[131] then the slow phosphate sorption observed in the former system could be caused by diffusion into the precipitate to convert $Al(OH)_3$ to $AlPO_4$. Similar processes may occur at low pH value on the surfaces of crystalline alumina.

Arsenate"' and boron[138–140] ddsorption reach equilibrium slowly. Silicate adsorption is also slow and may lead to polymerization on the aluminum hydroxide surface'"' or precipitation of an aluminum silicate.[142] Adsorption of fluoride, on the other hand, reaches equilibrium rapidly.[143,144]

Phosphate was found to interact specifically with the surface hydroxyls of gibbsite as observed using laser Raman spectroscopy.[145] Bleam et al.,[146] using NMR spectroscopy, observed that phosphate adsorbed on pseudoboehmite formed inner-sphere surface complexes.

Table 4 Adsorption of Inorganic Anions

Solid	Anions	Study type*	Ref.
γ-Al_2O_3	PO_4	a, b	119
γ-Al_2O_3	PO_4	a, b, e	124
γ-Al_2O_3	PO_4	a, j	158
γ-Al_2O_3	S_2O_3	a, b	215
γ-Al_2O_3	PO_4	a, j	101
γ-Al_2O_3	PO_4	a, c	125
γ-Al_2O_3	CrO_4	a, c, e	126
γ-Al_2O_3	F	a, b, c	144
δ-Al_2O_3	$B(OH)_4$	a	226
δ-Al_2O_3	$B(OH)_4$	a, b, c, j	155
α-Al_2O_3	PO,	a, b, j, k	128
α-Al_2O_3	PO,	c, g, h	131
α-Al_2O_3	PO,, CrO_4	a, i, j	123
α-Al_2O_3	PO_4	c	133
α-Al_2O_3	CrO_4	a, b, f, h	102
α-Al_2O_3	MoO_4	a, b	227
α-Al_2O_3	AsO_4	a, b, c, j	154
α-Al_2O_3	AsO_4, AsO_3	a, b, j	157
Al_2O_3	PO_4	a	228
Al_2O_3	$B(OH)_4$	a, c, i, j, k	140
Al_2O_3	F	a, b, c	143
Al_2O_3	F	a, b	229
Gibbsite	PO,	a, b, g	151, 230
Gibbsite	PO., AsO_4	a, b, j	117
Gibbsite	F, SO_4, SeO_3, MoO_4, $Si(OH)_4$	a, f	63
Gibbsite	PO_4	b, c	129
Gibbsite	PO_4	c	120
Gibbsite	PO4	b, c, k	132
Gibbsite	PO,, $Si(OH)_4$	d	145, 231
Gibbsite	$Si(OH)_4$	a, c, e	147
Gibbsite	PO_4	a, b	8
Gibbsite	PO,, $Si(OH)_4$	d	218
Gibbsite	PO_4	a, b, c, g	134,135
Gibbsite	F	a, b	229
Gibbsite	PO_4, AsO_4, MoO_4, SeO_3, CrO_4	a, b, f	232
Gibbsite	$Si(OH)_4$	b, c, g, h	142, 150
Gibbsite	$B(OH)_4$	a, b, e, g, i	149, 152
Bayerite	PO_4	b h	153
Boehmite	PO_4	a, d, e, f	146
Pseudoboehmite	PO_4	a, b, g	151, 230
Pseudoboehmite	$B(OH)_4$	e	148
Pseudoboehmite	$B(OH)_4$	a	226
$Al(OH)_3$	$Si(OH)_4$	a	233
$Al(OH)_3$	$Si(OH)_4$	a, b, c, f, i	141
$Al(OH)_3$	PO,	b, f	136
$Al(OH)_3$	PO,	c	137
$Al(OH)_3$	SeO_3	a	206, 221
$Al(OH)_3$	PO,	a	221
$Al(OH)_3$ gel	NO,, SO,, CO_3	d	234
$Al(OH)_3$ gel	$B(OH)_4$	d, e	213
$Al(OH)_3$ gel	PO_4	d	235
Hydrous Al_2O_3	PO_4, AsO_4, MoO_4, SeO_3, CrO_4	a, b, f	232
Hydrous Al_2O_3	PO_4	b, h	153

Table 4 (continued)

Solid	Anions	Study type*	Ref.
Amorphous $Al(OH)_3$	$B(OH)_4$	a, C	138
Amorphous $Al(OH)_3$	$B(OH)_4$, $Si(OH)_4$	a, c, j	139
Amorphous $Al(OH)_3$	AsO_4	a	236
Amorphous $Al(OH)_3$	AsO_4	a, b, c, e	122
Amorphous $Al(OH)_3$	PO,	b, c	133
Amorphous $Al(OH)_3$	PO_4 AsO_4	a, b, e	124
Amorphous $Al(OH)_3$	$B(OH)_4$	a	226
Amorphous $Al(OH)_3$	SO4	a, k	104
Amorphous $Al(OH)_3$	F	a, b	229
Amorahous $Al(OH)_3$	PO_4	a, b, j	156

* a, dependence on pH; b, dependence on anion concentration; c, kinetics; d, spectroscopy; e, electrokinetics; f, proton/hydroxyl release; g, dependence on temperature; h, dependence on suspension density; i, dependence on ionic strength; j, dependence on competing anion or ligand concentration; k, dependence on cation concentration.

The electrical charge on particles is decreased by strong anion adsorption. Several studies have shown that the i.e.p. of alumina suspensions is decreased by the adsorption of the anions arsenate,[122] phosphate,[124,146] silicate,[147] chromate,"' and borate.[148,149] Anderson and Malotky[124] have derived interesting isotherms as a function of i.e.p. for arsenate adsorption on $Al(OH)_3$ and for phosphate adsorption on γ-Al_2O_3. By separating out the influence of electrostatic forces, the authors attempted to derive the chemical energy of adsorption and maximum adsorption density from a linearized isotherm obtained at various i.e.p. values. They also demonstrated that electrophoretic mobilities can be described by one curve when plotted as a function of the reduced pH (pH-i.e.p.) in the presence of variable concentrations of arsenate and phosphate.

Anion sorption increases with increasing temperature when a precipitate is formed for phosphate[131,134] and silicate.[142,150] Adsorption of phosphate on gibbsite and pseudo-boehmite increases as a function of temperature because of an irreversible increase in the number of adsorption sites."' Boron adsorption on gibbsite is exothermic, decreasing with increasing temperature.^152

Anion adsorption is also a function of the suspension density of the adsorbent.[102,153] For a given total anion concentration, the adsorption envelope shifts to greater fractional surface coverage with increasing suspension density.^102 Adsorption of anions decreased with increasing ionic strength of the background electrolyte for chromate^123 and borate.^140,149 Silicate adsorption exhibited no ionic strength dependence for short reaction times and increased with increasing ionic strength after 50 d when polymerization on the surface occurred.^141 The presence of cations affects anion adsorption.[128,132,140]

Anion adsorption on aluminum oxides is affected by the presence of competing anions. Phosphate adsorption was decreased by arsenate adsorption on gibbsite^117 and by chromate adsorption on α-Al_2O_3.[123] The presence of sulfate decreased boron adsorption on aluminum oxide[140] and arsenate adsorption on α-Al_2O_3.[154] Boron adsorption was decreased by silicate adsorption on amorphous aluminum oxide,^139 aluminum oxide,[140] and δ-Al_2O_3.[155] Because the effect of silicate adsorption on boron adsorption was small, Goldberg and Glaubig[155] postulated that some adsorption sites exhibit anion preference.

The presence of organic ligands also affects anion adsorption on aluminum oxides. Phosphate adsorption decreased in the presence of oxalate on amorphous aluminum oxide[156] and on α-Al_2O_3 in the presence of oxalate, succinate, tartrate, and EDTA.[128] Fulvic acid depressed arsenate adsorption on α-Al_2O_3,[157] as did humic acid for phosphate adsorption on α-Al_2O_3.[128] Natural organic matter decreased phosphate adsorption on γ-Al_2O_3.[101,158]

VI. ADSORPTION OF ORGANIC LIGANDS

Organic acids exhibit adsorption behavior similar to that of inorganic anions on aluminum oxides and hydroxides (Table 5). Kummert and Stumm[12] reported on the adsorption of phthalate, salicylate, benzoate, and catechol on γ-Al_2O_3 as a function of pH. Adsorption of phthalate and salicylate was highly pH dependent; strong adsorption was observed at low pH. Benzoate was weakly adsorbed, indicating that the bidentate functionality of phthalate and salicylate molecules was an important factor in forming a strong bond at the surface. Catechol adsorption exhibited a different pattern, increasing with increasing pH. Kummert and Stumm[12] modeled the adsorption behavior as ligand-exchange reactions involving a single aluminol group and the deprotonated or singly protonated anion. In the case of catechol, it was presumed that the singly protonated anion formed the predominant surface complex. McBride and Wesselink[159] recently compared adsorption of catechol on gibbsite, boehmite, and amorphous aluminum hydroxide and found that the dominant crystal faces of gibbsite and boehmite were unreactive. Only singly coordinated aluminol groups on the edge faces of gibbsite were reactive, similar to observations made on phosphate adsorption.[8] IR spectroscopy suggested that the surface complex formed was a 1:1 bidentate complex of deprotonated catecholate with aluminum ions at the surface. These spectroscopic results suggest that the model-dependent conclusions concerning surface structure made by Kummert and Stumm[12] may need to be reexamined. Parfitt et al.[8] concluded that oxalate also formed a bidentate complex with singly coordinated aluminol sites on the edge faces of gibbsite.

The general pH dependence for adsorption of the organic acids is in good agreement with observations of dissolved organic carbon adsorption on γ-Al_2O_3[116,158,160] and adsorption of humic and fulvic acids on δ-Al_2O_3.[161] Both humic and fulvic acids show high affinity for the δ-Al_2O_3 surface; the stronger affinity for humic acid is ascribed to its higher hydrophobicity.[162,163] Fulvic and humic acids are adsorbed on gibbsite by ligand exchange at neutral pH; in acid solution additional adsorption occurs on the unreactive faces via hydrogen bonding.[164]

Huang and others[105,107,165] have conducted detailed studies of the adsorption of strongly complexing ligands (EDTA, NTA) and their metal complexes on γ-Al_2O_3 (Figure 16). Both EDTA and NTA adsorption increase with decreasing pH, similar to the adsorption behavior of phthalate and salicylate.[12] In homogeneous solution, EDTA forms hexadentate bonds with metal ions, generally using all its functional groups and coordination positions of the metal ion. At the surface, this is not possible without dissolution and detachment of the metal ion from the solid lattice. Surface complex formation involving more than one carboxylic group seems possible; however, Huang and coauthors[105,165] have explained their observations in terms of hydrogen bonding between aluminol groups and carboxylic groups of EDTA and NTA.

Table 5 Adsorption of Organic Ligands

Solid	Ligands	Study type*	Ref.
γ-Al_2O_3	NTA	a, b, k	105
γ-Al_2O_3	Catechol, salicylate, benzoate, phthalate	a,b,c,f	1 2
γ-Al_2O_3	Dissolved organic C	a, e	160
γ-Al_2O_3	Dissolved organic C	a, b e, h, i, j, k	158
γ-Al_2O_3	Dissolved organic C	a, b	116
γ-Al_2O_3	EDTA, DTPA, TTHA, EGTA, HEDTA, CDTA	a, e	165
γ-Al_2O_3	EDTA	a, e, g, k	106
γ-Al_2O_3	Dodecylsulfate	a, b, e, i, k	167
γ-Al_2O_3	Dinitrophenol	a, i	237
δ-Al_2O_3	Humic acid, fulvic acid	b	162
δ-Al_2O_3	Humic acid, methyloleate	a, b h	163
δ-Al_2O_3	Salicylate	a, e, f	46
δ-Al_2O_3	Heptylbenzenesulfonate, octylbenzenesulfonate	e	169
δ-Al_2O_3	Humic acid, fulvic acid	a	161
δ-Al_2O_3	EDTA	a, b k	108
α-Al_2O_3	Alkylsulfonates	b e	166
α-Al_2O_3	Dodecylsulfonate, lauric acid, oleic acid	e	168
α-Al_2O_3	Octylbenzenesulfonate	a, b	238
α-Al_2O_3	Octylbenzenesulfonate	a, b	239
η-Al_2O_3	Salicylate	a, e, f	46
η-Al_2O_3	Heptylbenzenesutfonate, octylbenzenesulfonate	e	169
Al_2O_3	Anionic dye Orange II	a, b	240
Al_2O_3	Ethoxylated sulfonates	b	241
Al_2O_3	Anionic dyes Trypan blue and Orange G	a, b	242
Al_2O_3	Octylbenzenesulfonate	a, b	238
Al_2O_3	Acetate	a, j	243
Al_2O_3	Maleic anhydride a-olefin copolymer	a, b e	244
Gibbsite	Polyvinyl alcohol	b e	54
Gibbsite	Oxalate, benzoate	a, b d	8, 164
Gibbsite	Humic acid, fulvic acid	a, b d	245
Gibbsite	Catechol, hydroquinone, phenol	b, d j	159
Gibbsite	Chlorophenols	b, d	246
Bayerite	Phenanthroline	a, b	247
Bayerite	Bipyridine	a, b	248
Bayerite	Quinoline	a	249
Boehmite	Catechol, hydroquinone, phenol	b d j	159
Pseudoboehmite	Citrate	a, b	214
Pseudoboehmite	Chlorophenols	b, d	246
$Al(OH)_3$ gel	Dodecylsulfonate, tetradecylsulfonate	a, b, c, e	250
$Al(OH)_3$ gel	Decanoate, dodecanoate	a, b, c, e	251
Hydrous Al_2O_3	Hydroxyquinoline	a, b c	252
Amorphous $Al(OH)_3$	Aspartate, glutamate	a, b	109
Amorphous $Al(OH)_3$	Phospho-serine, phospho-tyrosine	a b	253
Amorphous $Al(OH)_3$	Catechol, hydroquinone, phenol	b, d, j	159
Amorphous $Al(OH)_3$	Oxalate	a j	156

* a, dependence on pH; b, dependence on anion concentration; c, kinetics; d, spectroscopy; e, electrokinetics; f, proton/hydroxyl release; g, dependence on temperature; h, dependence on suspension density; i, dependence on ionic strength; j, dependence on competing anion or ligand concentration; k, dependence on cation concentration.

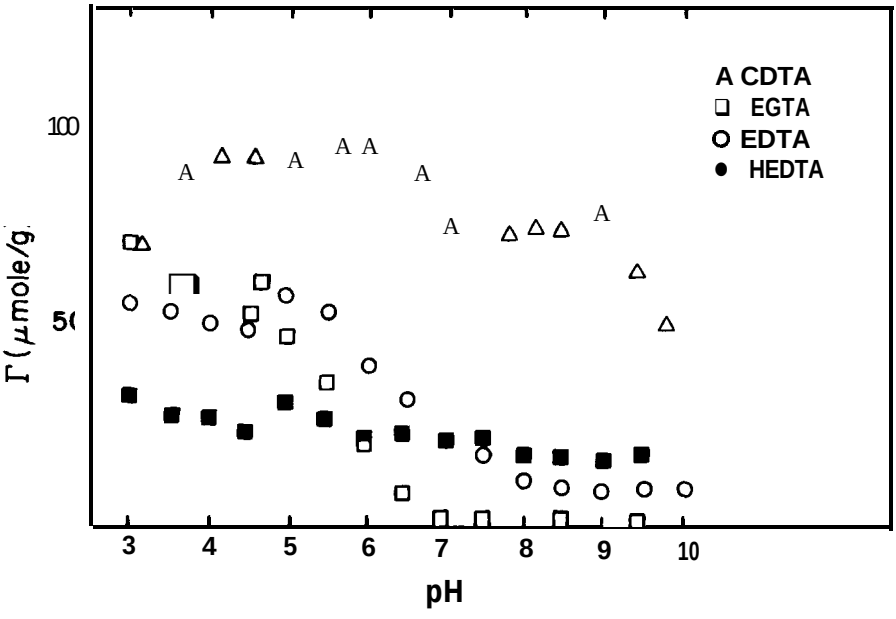

Figure 16 Adsorption of polyacetic amino acids on γ-Al_2O_3 from 0.025 mol dm ^{3} $NaClO_4$ solution as a function of pH. (From Bowers, A. R. and Huang, C. P., J. Colloid Interface Sci., 105, 197, 1985. With permission.)

Surfactant adsorption on aluminum oxides has been investigated by various researchers.[166,167] Adsorption isotherms correspond to three regions of increasing surfactant concentration. In region 1 the surfactant ions adsorb in competition with the background electrolyte ions. In region 2 the surfactant ions associate into aggregates called hemicelles resulting in a sharp increase in adsorption density. In region 3 the adsorption isotherm starts to decrease because of a reversal in surface charge.[166,167] Surfactant molecules can be adsorbed on aluminum oxides via a combination of electrostatic interaction, specific adsorption, and ion exchange.[168,169]

VII. PRECIPITATION OF ALUMINUM OXIDES AND HYDROXIDES

The hydrolysis of aluminum in aqueous systems has received much attention in the past few decades as researchers have attempted to understand the complicated processes of polymerization and precipitation of aluminum oxides and hydroxides. These processes are discussed in detail in other chapters of this volume, especially in Chapter 4. A brief review also is presented here to emphasize the interrelated nature of surface chemistry and precipitation.

The hydrolysis and precipitation of aluminum from unseeded, acidic solutions has been shown to produce three general types of species: (1) monomeric aluminum hydroxide complexes, (2) polynuclear or polymeric aluminum hydroxide complex ions, and (3) crystalline or microcrystalline gibbsite.[2,9,170–173] The relative proportions of these

species depend upon the conditions during hydrolysis (e.g., pH value, Al^{3+} concentration) and age of the hydrolysis products.[9,171–173] Under some conditions, much of the dissolved aluminum may be present as polymeric ions with a considerable range of composition and structure, and some of these species may persist for a long time.[9,171,174] A significant degree of supersaturation is required to produce microcrystalline gibbsite from unseeded solutions,[15,175] but the crystal growth reaction may proceed at lower reaction affinities in the presence of a surface that is favorable for nucleation. If the initial surface is gibbsite, a reversible solubility equilibrium controlled by a well-crystallized form of gibbsite may be attained at 25°C in 422 h or less.'"

van Straten and others"',"' have studied the precipitation of aluminum hydroxide phases from basic aqueous solutions. A precipitation sequence was observed in which the thermodynamically least stable phase was usually the first to form, followed by transformation to other phases in stages, i.e., amorphous aluminum hydroxide, pseudo-boehmite, bayerite, and gibbsite. The growth of bayerite was retarded by the presence of pseudoboehmite. The authors concluded that pseudoboehmite formation was favored at relatively high (but still alkaline) pOH values, and that this phenomenon was related to the lower interfacial tension of pseudoboehmite in comparison to bayerite. A two-dimensional nucleation mechanism was proposed as the rate-determining step for bayerite formation. The growth rate of bayerite was proportional to the available surface area and the square of the degree of supersaturation. The rate of transformation of bayerite to gibbsite increased with increasing temperature or with decreasing pOH values. These studies clearly demonstrated the role of surface chemical behavior in nucleation and crystal growth processes.

It should be apparent that the specific surface area of a precipitate will be influenced by the size of particles formed. Calculations of the surface energy of microcrystalline gibbsite suggest that the difference in solubility between this material and well-crystallized gibbsite can be accounted for by the difference in particle size and hence the difference in surface energy per unit mass of material.[178] Parthasarathy and Buffle[173] found that a substantial fraction of the microcrystalline gibbsite formed in their experiments was removed by an ultrafilter with pores 13 nm in diameter. The remaining material was removed by a filter having pores of 2 nm in diameter. These dimensions are within the general range of minimum particle size for microcrystalline gibbsite calculated by Smith and Hem.' Using the gibbsite structural model (Figure 5) and assuming all OH is present in bridging positions, a single sheet of $Al(OH)_6$ octahedra with this composition would be 50 to 100 Å units in diameter. Stacking of the layers might decrease the lateral dimension by a factor of two or more, but the particle size would still be within the general range indicated by the ultrafiltration experiments.

A. INFLUENCE OF ADSORPTION ON PRECIPITATION

As discussed in detail in Chapter 4, a number of different anions may perturb the precipitation of aluminum and lead to the formation of noncrystalline products or poorly crystalline pseudoboehmite."' Hsu[180] found that several inorganic ligands inhibited the crystallization of aluminum hydroxide. Numerous investigations have also shown this effect when precipitation occurs in the presence of organic ligands.[181–184] These results demonstrate that interactions between adsorbing anions and the coalescing polymers may influence the type of precipitate formed.

B. COPRECIPITATION AND ADSORPTION IN NATURAL SYSTEMS

In laboratory experiments it is possible to maintain conditions that will prevent extensive alterations and recrystallization of an $Al(OH)_3$ solid, but natural systems are not this simple. For that reason it may be necessary to allow for coprecipitation effects in evaluating the surface properties of naturally occurring $Al(OH)_3$ solids.

In all the specific interactions mentioned above it is necessary to consider relationships to the aluminum hydroxide polymerization process. If the polymerization has gone essentially to completion so that only a form of crystalline gibbsite and monomeric aluminum ions are present, the extent of incorporation of other ions into the solid phase will depend primarily on the extent to which the surface may be undergoing alteration. In natural systems there will generally be changes in pH, temperature, and concentrations of various solutes as water moves past the surface and dissolution and reprecipitation reactions can be expected.

C. INFLUENCE OF ADSORPTION ON DISSOLUTION

Zutic and Stumm[185] have conducted an interesting study of the influence of adsorption on the rates of aluminum oxide and hydroxide dissolution. These authors proposed that the rate of dissolution was controlled by a surface process in the presence of organic ligands and at low pH. The detachment of surface complexes was thought to be the rate-controlling step in the dissolution process. Fluoride ions increased the dissolution rate dramatically at concentrations as low as 10^{-6} mol dm^{-3}. Furrer and Stumm[186] showed that the adsorption of various organic ligands promoted dissolution of δ-Al_2O_3. Organic ligands capable of forming surface chelates were especially effective. For the dicarboxylic acids, oxalate, which forms a five-membered ring, was more effective in increasing the dissolution rate than malonate, forming a six-membered ring, and succinate, forming a seven-membered ring. Similarly, for the aromatic ligands, salicylate, forming a six-membered chelate ring, was more effective than phthalate, which forms a seven-membered ring.[186]

VIII. ADSORPTION MODELS FOR ALUMINUM OXIDES AND HYDROXIDES

Quantitative models for the surface chemistry of oxides have evolved substantially during the last two decades. The *surface complexation models,* which describe the formation of charge, potential, and the adsorption of ions at the oxide-water interface, are the most popular. The fundamental concept upon which all surface complexation models are based is that adsorption takes place at defined coordination sites (the surface hydroxyl groups, present in finite number) and that adsorption reactions can be described quantitatively via mass action equations (e.g., Equations I, 2, 6 to 8, and 13 to 17).[187] Various models can be distinguished on the basis of different assumptions made for electrostatic interaction terms, or more correctly, surface activity coefficients.[188] However, all of these models reduce to a similar set of simultaneous equations that can be solved numerically, including: (I) mass action equations for all surface reactions; (2) a mass balance equation for surface hydroxyl groups; (3) equations for calculation of

surface charge; (4) a set of equations that describes the charge and potential relationships of the electrical double layer.[187]

A. CONSTANT CAPACITANCE MODEL

The constant capacitance mode1 was developed by the research groups of Schindler and Stumm.[90,189–192] The mode1 is based on the following assumptions: (1) ion adsorption is based on a ligand exchange mechanism; (2) all surface complexes are inner-sphere complexes; (3) no surface complexes are formed with ions from the background electrolyte; (4) the relationship between surface charge and surface potential is linear:

$$\sigma = \frac{CSa}{F}\psi \tag{18}$$

where C is the capacitance density (F m^{-2}), S is the surface area (m^2 g^{-1}), a is the suspension density (g l^{-1}), and σ has units of mol, l^{-1}. A diagram of the surface-solution interface for the constant capacitance model is provided in Figure 17.

The equations for the inner-sphere surface complexation reactions include Equations 1 and 2 for protonation-dissociation, and[193]

$$\mathrm{AlOH} + \mathrm{M}^{m+} \rightleftarrows \mathrm{AlOM}^{(m-1)} + \mathrm{H}^{+} \tag{19}$$

$$2\mathrm{AlOH} + \mathrm{M}^{m+} \rightleftarrows (\mathrm{AlO})_2\mathrm{M}^{(m-2)} + 2\mathrm{H}^{+} \tag{20}$$

$$\mathrm{AlOH} + \mathrm{L}^{\ell} \rightleftarrows \mathrm{AlL}^{(\ell-1)-} + \mathrm{OH}^{-} \tag{21}$$

$$2\mathrm{AlOH} + \mathrm{L}^{\ell} \rightleftarrows \mathrm{Al_2L}^{(\ell-2)-} + 2\mathrm{OH}^{-} \tag{22}$$

where AlOH represents the surface functional group, M is a metal ion, m^+ is the charge on the metal ion, L is a ligand, and ℓ^- is the charge on the ligand.

The intrinsic conditional equilibrium constants describing protonation-dissociation and the above reactions are[193]

$$K_{+}(\mathrm{int}) = \frac{[\mathrm{AlOH_2^+}]}{[\mathrm{AlOH}][\mathrm{H^+}]}\exp[F\psi/RT] \tag{23}$$

$$K_{-}(\mathrm{int}) = \frac{[\mathrm{AlO^-}][\mathrm{H^+}]}{[\mathrm{AlOH}]}\exp[-F\psi/RT] \tag{24}$$

$$K_{\mathrm{M}}^{1}(\mathrm{int}) = \frac{[\mathrm{AlOM}^{(m-1)}][\mathrm{H^+}]}{[\mathrm{AlOH}][\mathrm{M}^{m+}]}\exp[(m-1)F\psi/RT] \tag{25}$$

$$K_{\mathrm{M}}^{2}(\mathrm{int}) = \frac{[(\mathrm{AlO})_2\mathrm{M}^{(m-2)}][\mathrm{H^+}]^2}{[\mathrm{AlOH}]^2[\mathrm{M}^{m+}]}\exp[(m-2)F\psi/RT] \tag{26}$$

$$K_{\mathrm{L}}^{1}(\mathrm{int}) = \frac{[\mathrm{AlL}^{(\ell-1)-}][\mathrm{OH^-}]}{[\mathrm{AlOH}][\mathrm{L}^{\ell-}]}\exp[-(\ell-1)F\psi/RT] \tag{27}$$

$$K_{\mathrm{L}}^{2}(\mathrm{int}) = \frac{[\mathrm{Al_2L}^{(\ell-2)-}][\mathrm{OH^-}]^2}{[\mathrm{AlOH}]^2[\mathrm{L}^{\ell-}]}\exp[-(\ell-2)F\psi/RT] \tag{28}$$

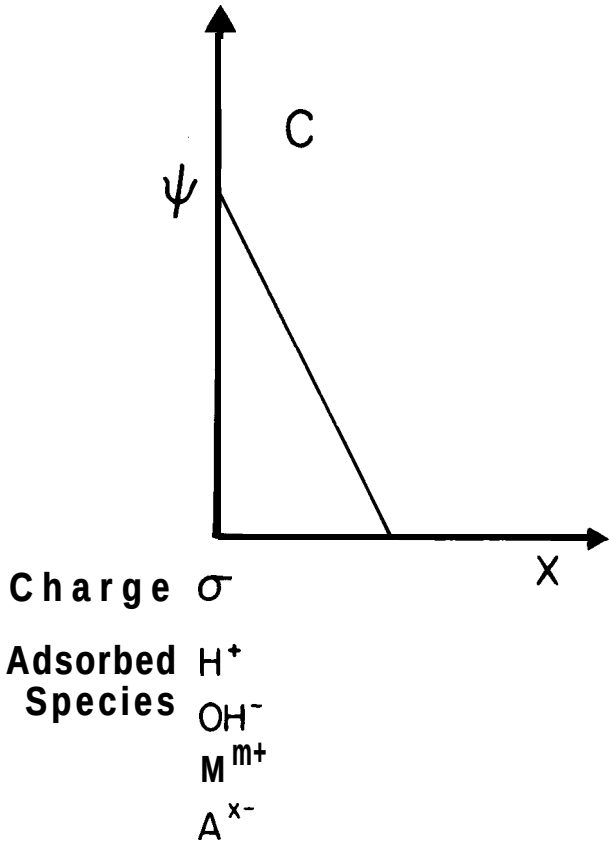

Figure 17 Placement of ions, potential, charge, and capacitance for the constant capacitance model. (Modified from Westall, J. C., *Am. Chem.Soc. Symp. Ser., 323, 54,* 1986.)

where R is the molar gas constant (J $mol^{-1}K^{-1}$), T is the absolute temperature (K), and square brackets represent concentrations (mol I-'). Experimental values of the intrinsic conditional equilibrium constants can be obtained by extrapolating the conditional equilibrium constants to zero net surface charge, as described in detail by Stumm et al.[192] Such extrapolations also yield values of the capacitance density, C.

The mass balance expression for the surface functional group, AlOH, is

$$[\mathrm{AlOH}]_T = [\mathrm{AlOH}] + [\mathrm{AlOH_2^+}] + [\mathrm{AlO^-}] + [\mathrm{AlOM^{(m-1)}}] + 2[(\mathrm{AlO})_2\mathrm{M^{(m-2)}}] + [\mathrm{AlL^{(\ell-1)-}}] + 2[\mathrm{Al_2L^{(\ell-2)-}}] \quad (29)$$

and the charge balance expression is

$$\sigma = [\mathrm{AlOH_2^+}] - [\mathrm{AlO^-}] + (m-1)[\mathrm{AlOM^{(m-1)}}] + (m-2)[(\mathrm{AlO})_2\mathrm{M^{(m-2)}}] \quad (\ell-1)[\mathrm{AlL^{(\ell-1)-}}] - (\ell-2)[\mathrm{Al_2L^{(\ell-2)-}}] \quad (30)$$

Table 6 Applications of the Constant Capacitance Model to ion Adsorption

Solid	Ions	Ref.
γ-Al_2O_3	H, OH, Ca, Mg, Sr, Ba	53
γ-Al_2O_3	H, OH, Pb	90
γ-Al_2O_3	H, OH	254
γ-Al_2O_3	H, OH, catechol, salicylate, benzoate, phthalate	12
γ-Al_2O_3	H, OH, SO_4	193
γ-Al_2O_3[a]	PO_4	255
δ-Al_2O_3	$B(OH)_4$	226
δ-Al_2O_3	$B(OH)_4$, $Si(OH)_4$	155
α-Al_2O_3[a]	PO,	255
α-Al_2O_3	H, OH	256
Al_2O_3	$B(OH)_4$	257
Al_2O_3	H, OH, Cd, Zn, SeO_3	206
Gibbsite[a]	PO4	255
Gibbsite[a]	SeO_3	257
Gibbsite"	AsO_4	258
Gibbsite	$B(OH)_4$	149
Bayerite	H, OH	259
Boehmite	H, OH, PO_4	146
Pseudobeohmite	$B(OH)_4$	226
Pseudoboehmite	H, OH, citrate	214
Hydrous Al_2O_3[a]	PO_4	255
Amorphous $Al(OH)_3$	$B(OH)_4$	226
Amorphous $Al(OH)_3$[a]	AsO_4	257,258

[a] Experimental data source provided in the reference

The constant capacitance model has been used to describe proton, hydroxyl, metal, and ligand adsorption data. Table 6 lists the various studies that have applied the constant capacitance model to ion adsorption. Since the model uses the constant ionic medium reference state it cannot describe adsorption as a function of ionic strength. Application of the mode1 is restricted to specifically adsorbing ions forming strong inner-sphere complexes and showing little ionic strength dependence in their adsorption behavior.

B. TRIPLE LAYER MODEL

The original triple layer model was developed by Davis and co-workers[52,92,121] as an extension of the site binding model'" and subsequently modified to include inner-sphere surface complexation reactions.[194,195] The model is based on the following assumptions: (I) protons and hydroxyl ions form inner-sphere complexes; (2) ion adsorption reactions form either outer-sphere or inner-sphere complexes; (3) outer-sphere surface complexes are formed with ions from the background electrolyte; (4) three planes of charge represent the surface; (5) the relationships between surface charges and surface potentials are

$$\psi_0 - \psi_\beta = \sigma_0/C_1 \tag{31}$$

$$\psi_\beta - \psi_d = -\sigma_d/C_2 \tag{32}$$

$$\sigma_d = -(8RTc\epsilon_0 D)^{1/2}\sinh(F\psi_d/2RT) \tag{33}$$

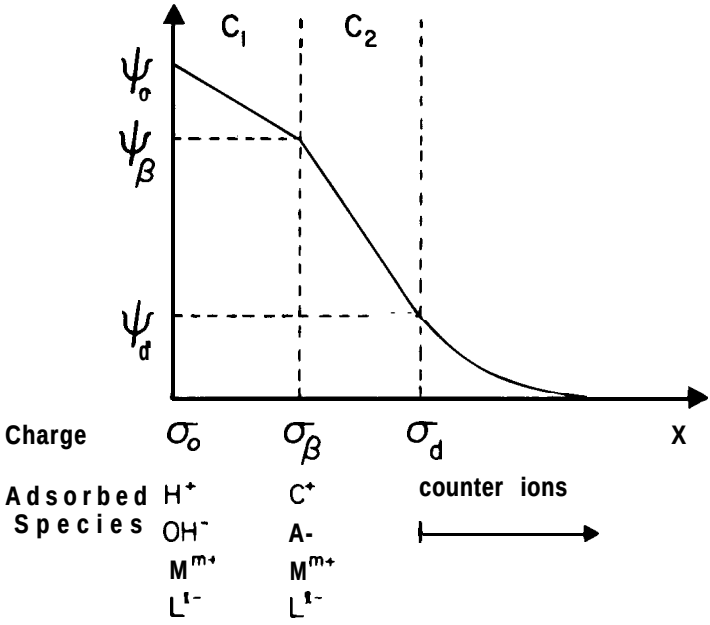

Figure 18 Placement of ions, potentials, charges, and capacitances for the triple layer model. (Modified from Westall, J., *Am. Chem. Soc. Adv. Chem. Ser.,* 189, 33, 1980.)

where ϵ_o is the permittivity of vacuum, D is the dielectric constant of water, c is the concentration of a 1: 1 background electrolyte, and σ has units of C m^{-2}. A diagram of the surface-solution interface for the triple layer model is provided in Figure 18.

The equations for the inner-sphere surface complexation reactions in the triple layer model are Equations 1 and 2 and Equations 19 through 22 as written for the constant capacitance model. The equations for the outer-sphere surface complexation reactions are[52,92,121]

$$AlOH + M^{m+} \rightleftarrows AlO^- - M^{m+} + H^+ \quad (34)$$

$$AlOH + M^{m+} + H_2O \rightleftarrows AlO^- - MOH^{(m-1)} + 2H^+ \quad (35)$$

$$AlOH + H+ + L^{\ell-} \rightleftarrows AlOH_2^+ - L^{\ell-} \quad (36)$$

$$AlOH + 2H^+ + L^{\ell-} \rightleftarrows AlOH_2^+ - LH^{(\ell-1)-} \quad (37)$$

$$AlOH + C^+ \rightleftarrows AlO^- - C^+ + H+ \quad (38)$$

$$AlOH + H^+ + A^- \rightleftarrows AlOH_2^+ - A^- \quad (39)$$

where C^+ is the cation and A^- is the anion of the background electrolyte.

The intrinsic conditional equilibrium constants for the triple layer model are Equations 23 through 28 as written for the constant capacitance model for inner-sphere surface

complexation with ψ equal to ψ_o. For outer-sphere surface complexation the intrinsic conditional equilibrium constants are[52,92,121]

$$K_M^1(\text{int}) = \frac{[\text{AlO}^- - \text{M}^{m+}][\text{H}^+]}{[\text{AlOH}][\text{M}^{m+}]} \exp[\text{F}(m\psi_\beta - \psi_0)/\text{RT}] \quad (40)$$

$$K_M^2(\text{int}) = \frac{[\text{AlO}^- - \text{MOH}^{(m-1)}][\text{HN}^+]^2}{[\text{AlOH}][\text{M}^{m+}]} \exp[\text{F}((m-1)\psi_\beta - \psi_0)/\text{RT}] \quad (41)$$

$$K_L^1(\text{int}) = \frac{[\text{AlOH}_2^+ - \text{L}^{\ell-}]}{[\text{AlOH}][\text{H}^+][\text{L}^{\ell-}]} \exp[\text{F}(\psi_0 - \ell\psi_\beta)/\text{RT}] \quad (42)$$

$$K_L^2(\text{int}) = \frac{[\text{AlOH}_2^+ - \text{LH}^{(\ell-1)-}]}{[\text{AlOH}][\text{H}^+]^2[\text{L}^{\ell-}]} \exp[\text{F}(\psi_0 - (\ell-1)\psi_\beta)/\text{RT}] \quad (43)$$

$$K_{C^+}(\text{int}) = \frac{[\text{ALO}^- - \text{C}^+][\text{H}^+]}{[\text{AlOH}][\text{C}^+]} \exp[\text{F}(\psi_\beta - \psi_0)/\text{RT}] \quad (44)$$

$$K_{A^-}(\text{int}) = \frac{[\text{AlOH}_2^+ - \text{A}^-]}{[\text{AlOH}][\text{H}^+][\text{A}^-]} \exp[\text{F}(\psi_0 - \psi_\beta)/\text{RT}] \quad (45)$$

As for the constant capacitance model, experimental values for the intrinsic conditional equilibrium constants can be obtained by extrapolation. A detailed explanation of the various types of extrapolation procedures used for the triple layer model is provided by Goldberg.[196] These extrapolations also yield values of the capacitance density, C,. An experimental value of the capacitance density, C_2, can be obtained only from the Sprycha electrokinetic extrapolation.[45,197]

The mass balance equation for the surface functional group, AlOH, is

$$\begin{aligned}[\text{AlOH}]_T = {} & [\text{AlOH}] + [\text{ALOH}_2^+] + [\text{AlO}^-] + [\text{AlOM}^{(m-1)}] \\ & + 2[(\text{AlO})_2\text{M}^{(m-2)}] + [\text{AlL}^{(\ell-1)-}] + 2[\text{Al}_2\text{L}^{(\ell-2)-}] \\ & + [\text{AlO}^- - \text{M}^{m+}] + [\text{AlO}^- - \text{MOH}^{(m-1)}] + [\text{AlOH}_2^+ - \text{L}^{\ell-}] \\ & + [\text{AlOH}_2^+ - \text{LH}^{(\ell-1)-}] + [\text{AlO}^- - \text{C}^+] + [\text{AlOH}_2^+ - \text{A}^-] \end{aligned} \quad (46)$$

and the charge balance equations are

$$\sigma_0 + \sigma_\beta + \sigma_d = 0 \quad (47)$$

$$\begin{aligned}\sigma_0 = {} & \frac{\text{F}}{Sa}\{[\text{AlOH}_2^+] + [\text{AlOH}_2^+ - \text{L}^{\ell-}] + [\text{AlOH}_2^+ - \text{LH}^{(\ell-1)-}] \\ & + (m-1)[\text{AlOM}^{(m-1)}] + (m-2)[(\text{AlO})_2\text{M}^{(m-2)}] \\ & + [\text{AlOH}_2^+ - \text{A}^-] - [\text{AlO}^-] - [\text{AlO}^- - \text{M}^{m+}] \\ & - [\text{AlO}^- - \text{MOH}^{(m-1)}] - (\ell-1)[\text{AlL}^{(\ell-1)-}] \\ & - (\ell-2)[\text{Al}_2\text{L}^{(\ell-2)-}] - [\text{AlO}^- - \text{C}^+]\} \end{aligned} \quad (48)$$

Table 7 Applications of the Triple Layer Model to Ion Adsorption

Solid	Ions	Ref.
γ-Al_2O_3	H, OH, Pb, Cd, Cu, Zn	92
γ-Al_2O_3	H, OH	254
γ-Al_2O_3	H, OH	67
γ-Al_2O_3	PO4	125
γ-Al_2O_3	CrO_4	126
γ-Al_2O_3	H, OH, Na, Cl	45, 197
α-Al_2O_3	Na, Br	17
α-Al_2O_3	CrO_4	260
α-Al_2O_3	H, OH, Na, NO_3	256
Boehmite	H, OH, K, NO_3	47

$$\sigma_\beta = \frac{F}{Sa}\{m[AlO^- - M^{m+}] + (m-1)[AlO^- - MOH^{(m-1)}] + [AlO^- - C^+] - \ell[AlOH_2^+ - L^{\ell-}] - (\ell-1)[AlOH_2^+ - LH^{(\ell-1)-}] - [AlOH_2^+ - A^-]\} \quad (49)$$

The triple layer model has been used to describe proton, hydroxyl, metal, and ligand adsorption data. Table 7 lists various applications of the triple layer model to ion adsorption. The model uses the infinite dilution reference state and thus can describe adsorption as a function of ionic strength.

C. ONE-pK MODEL

The one-pK model was developed by van Riemsdijk and co-workers.[41,198–201] In the one-pK concept the surface functional group is defined as a singly coordinated oxygen atom that carries either one or two protons leading to surface sites AlOH and $AlOH_2$, respectively. The constant capacitance model and the triple layer model could be written based on the one-pK concept for singly coordinated oxygen atoms. The Stern model of the surface-solution interface has been chosen as the basis for the one-pK model.“’ The model is based on the following assumptions: (I) protons and hydroxyl ions form inner-sphere surface complexes; (2) cations and anions form outer-sphere surface complexes; (3) the relationships between surface charges and surface potentials are Equation 33 and[200]

$$\sigma_0 = C(\psi_0 - \psi_d) \quad (50)$$

where the units of σ are C m^{-2}. A diagram of the surface-solution interface for the one-pK model is provided in Figure 19.

The surface complexation reactions[199–201]

$$AlOH^{1/2-} + H^+ \rightleftarrows AlOH_2^{1/2+} \quad (51)$$

$$AlOH^{1/2-} + M^{m+} \rightleftarrows AlOH^{1/2-} - M^{m+} \quad (52)$$

$$AlOH^{1/2-} + M^{m+} + H_2O \rightleftarrows AlOH^{1/2-} - MOH^{(m-1)} + H+ \quad (53)$$

$$AlOH_2^{1/2+} + L^{\ell-} \rightleftarrows AlOH_2^{1/2+} - L^{\ell-} \quad (54)$$

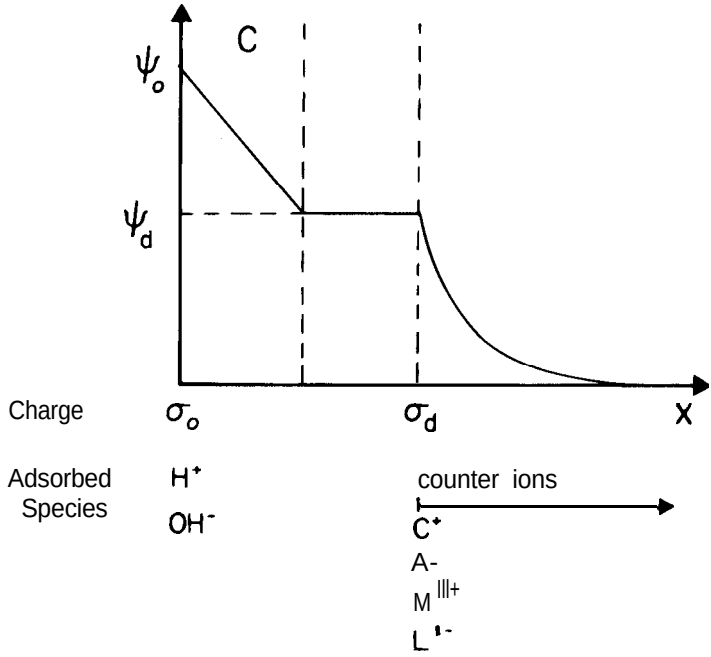

Figure 19 Placement of ions, potentials, charges, and capacitance for the one-pK model. (Modified from Westall, J. C., *Am. Chem. Soc. Symp. Ser., 323, 54,* 1986.)

$$AlOH^{1/2-} + C^+ \rightleftarrows AlOH^{1/2-} - C+ \tag{55}$$

$$AlOH_2^{1/2+} + A^- \rightleftarrows AlOH_2^{1/2+} - A^- \tag{56}$$

The intrinsic equilibrium constants are[199–201]

$$K_H = \frac{[AlOH_2^{1/2+}]}{[AlOH^{1/2-}][H^+]} \exp[F\psi_0/RT] \tag{57}$$

$$K_M^1 = \frac{[AlOH^{1/2-} - M^{m+}]}{[AlOH^{1/2-}][M^{m+}]} \exp[mF\psi_d/RT] \tag{58}$$

$$K_M^2 = \frac{[AlOH^{1/2-} - MOH^{(m-1)}][H^+]}{[AlOH^{1/2-}][M^{m+}]} \exp[(m-1)F\psi_d/RT] \tag{59}$$

$$K_L = \frac{[AlOH_2^{1/2+} - L^{\ell-}]}{[AlOH_2^{1/2+}][L^{\ell-}]} \exp[-\ell F\psi_d/RT] \tag{60}$$

$$K_{C^+} = \frac{[AlOH^{1/2-} - C^+]}{[AlOH^{1/2-}][C^+]} \exp[F\psi_d/RT] \tag{61}$$

$$K_{A^-} = \frac{[AlOH_2^{1/2+} - A^-]}{[AlOH_2^{1/2+}][A^-]} \exp[-F\psi_d/RT] \quad (62)$$

The mass balance of singly coordinated oxygen atoms N_S, is

$$N_S = [AlOH^{1/2-}] + [AlOH_2^{1/2+}] \quad (63)$$

The surface charge balance equation is

$$\sigma_0 = 1/2\ [AlOH_2^{1/2+} - AlOH^{1/2-}] \quad (64)$$

The one-pK model has been used to describe potentiometric titration data for gibbsite and γ-Al_2O_3 in inert background electrolyte solution.[200] In the most simplified application of the one-pK model, no surface complexation reactions are considered for the background electrolyte and the capacitance density of the Stern layer is the only adjustable parameter. The association constant K_H is obtained from the p.z.c.:

$$\log K_H = pH_0 = \text{p.z.c.} \quad (65)$$

where pH_0 is the proton concentration at the p.z.c.[41] Titration data on gibbsite were modeled successfully in this fashion.“” The model fit can be improved by inclusion of surface complexation constants for the background electrolyte. Hiemstra et al.[200] were able to describe potentiometric titration data well on gibbsite with both approaches. The model fit obtained by neglecting the surface complexation constants for the background electrolyte was good, but resulted in a low capacitance value. A larger capacitance value was obtained using surface complexation constants for the background electrolyte and the assumption that only the edge surface area of gibbsite is reactive. The one-pK model has not yet been applied to describe metal or ligand adsorption on aluminum oxide minerals.

Two-pK models, such as the constant capacitance and the triple layer model, and the one-pK model are special cases of a more generalized model called the MultiSite Complexation, MUSIC, model developed by Hiemstra et al.[202,203] This model considers equilibrium constants for the various types of surface groups on the various crystal planes of oxide minerals and was used to describe the charging behavior of gibbsite.[203] The MUSIC model has not yet been applied to describe ion adsorption. Because of its increased complexity such an application may result in an unreasonably large number of adjustable parameters.

D. USE OF SURFACE COMPLEXATION MODELS IN THE DESCRIPTION OF MINERAL DISSOLUTION

The dissolution kinetics of most aluminum oxides are controlled by chemical surface processes.[186] The reaction steps are (1) attachment of the reactants at surface sites, (2) rate-limiting detachment of the surface aluminum species, (3) transport of the aluminum complex into the bulk solution, (4) regeneration of the active site by protonation. Under acid conditions the dissolution is promoted by protons binding to the surface oxide ions.[186] The proton-promoted aluminum oxide dissolution rate is[204]

$$R_H = k_H[AlOH_2^+]^n = k_H(C_H^s)^n \quad (66)$$

where k_H is the rate constant, C_H^s is the surface proton concentration in mol m^{-2}, and

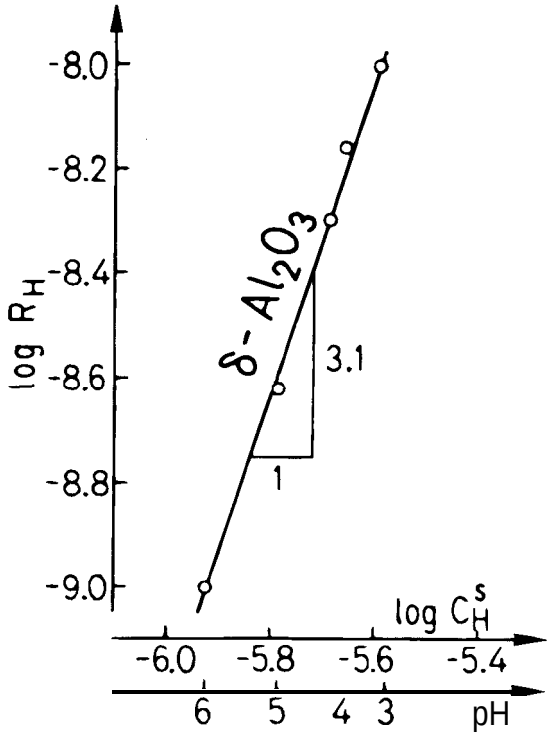

Figure 20 Dependence of the rate of the proton-promoted dissolution of δ-Al_2O_3. (From Stumm, W. and Wollast, R., Rev. Geophys., 28, 53, 1990; data from Furrer, G. and Stumm, W., *Geochim. Cosmochim.* Acta, 50, 1847, 1986.)

n is the number of protonation steps in the dissolution mechanism. The concentration of protonated surface hydroxyl groups, $[AlOH_2^+]$ is obtained using the constant capacitance model. In the presence of complex-forming ligands the aluminum oxide dissolution is promoted by ligands that form surface complexes by ligand exchange.[186] The ligand-promoted aluminum oxide dissolution rate is[204]

$$R_L = k_L[AlL] = k_L C_L^s \tag{67}$$

where k_L is the rate constant and C_L^s is the concentration of adsorbed ligand in mol m^{-2}. The concentration of surface sites occupied by ligand, [AIL], is obtained using the constant capacitance model. If the proton-promoted and the ligand-promoted dissolution are independent and parallel the total aluminum oxide dissolution rate is additive:^186

$$R_{tot} = R_H + R_l \tag{68}$$

Figure 20 indicates the dependence of the rate of the proton-promoted dissolution of δ-Al_2O_3 on the surface concentration of protons. The slope is close to 3, indicating that *n* is equal to 3 for δ-Al_2O_3. Furrer and Stumm[186] suggest that the reaction order *n* may correspond to the oxidation number of the aluminum ion in the oxide mineral. The

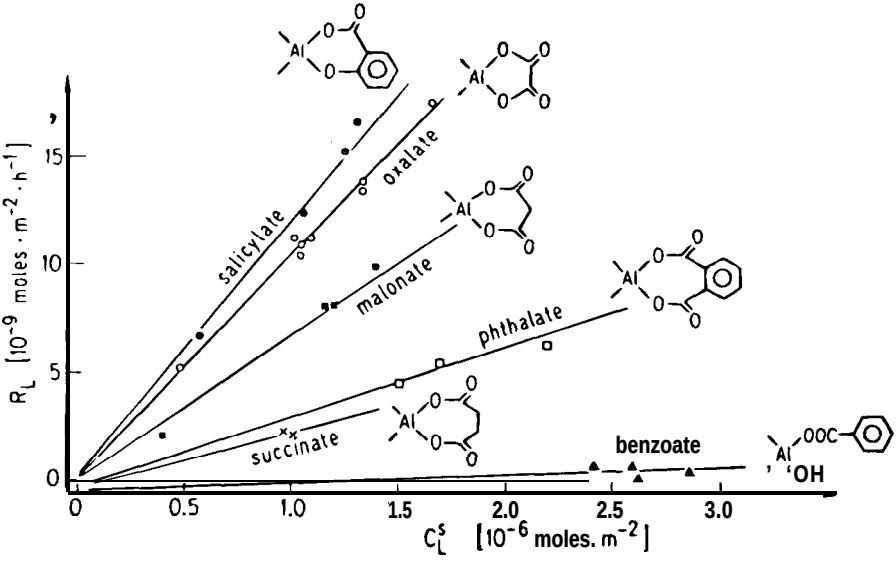

Figure 21 Dependence of the rate of the ligand-promoted dissolution of δ-Al_2O_3 on the surface concentration of ligands. (From Stumm, W., Wehrli, B., and Wieland, E., *Croatica Chem. Acta,* 60, 429, 1987; data from Furrer, G. and Stumm, W., Geochim. Cosmochim. *Acta, 50,* 1947, 1986.)

dependence of the rate of the ligand-promoted dissolution of δ-Al_2O_3 on the surface concentration of organic ligands is indicated in Figure 21.

IX. CONCLUDING REMARKS

Knowledge of the surface chemical behavior of aluminum oxides and hydroxides is still advancing. More is known in terms of systematic laboratory studies about the synthetic material, γ-Al_2O_3, than any other phase. The results of experimental studies of the gibbsite surface are consistent with what is expected in terms of the exposure of different crystal faces as predicted from the crystal structure. Little is known regarding the effects of surface alteration on the observed surface chemical behavior. More systematic and comprehensive studies of gibbsite are needed.

Recent advances, such as the measurement of surface potential as a function of pH and studies of the specific adsorption of counterions such as Na^+ and Br^-, are affecting dramatically the evolution of models for the alumina-water interface. However, models for the adsorption of solutes from dilute solutions have not yet been combined in a consistent way with spectroscopic studies of the surface. Much more research also is needed on the kinetics of adsorption reactions, the determination of maximum adsorption densities, the stoichiometry of surface reactions, and the ionic strength dependence of adsorption reactions. Although model development and the experimental studies conducted to date represent a considerable increase in knowledge, quantitative application of this knowledge to the natural environment still appears problematic. Furthermore, a

greater understanding of the role of adsorption in the precipitation process and the rates at which the surfaces of metastable minerals are altered by reorganization is required to improve geochemical models.

ACKNOWLEDGMENTS

Gratitude is expressed to Mr. H. Forster for library assistance, Ms. P. Speckman for typing, and Ms. S. Kao for drafting.

REFERENCES

I. Lippens, B. C. and Steggerda, J. J., Active alumina, in Physical *and Chemical Aspects of Adsorbents and Catalysts,* Linsen, B. G., Ed., Academic Press, New York, 1970, chap. 4.

2. Hsu, P. H., Aluminum hydroxides and oxyhydroxides, in *Minerals in Soil Environments,* Dixon, J. B., et al., Eds., Soil Science Society of America, Madison, WI, 1977, 99.

3. Wefers, K. and Misra, C., Oxides and hydroxides of aluminum, Tech. Paper No. 19, Rev., Alcoa Research Laboratories, Alcoa Center, PA, 1987.

4. May, H. M., The hydrolysis of aluminum: conflicting models and the interpretation of aluminum geochemistry, Proceedings of the 7th International Symposium on Water-Rock Interaction-WRI 7, Kharaka, Y. and Maest, A., Eds., Vol. I, A. A. Balkema, Rotterdam, MD, 1992, 13.

5. Davis, J. A. and Hayes, K. F., Geochemical processes at mineral surfaces: an overview, in *Geochemical Processes at Mineral Surfaces,* ACS Symp. Ser. 323, Davis, J. A. and Hayes, K. F., Eds., American Chemical Society, Washington, D.C., 1986, chap. I

6. Peri. J. B., A model for the surface of y-alumina, J. *Phys. Chem., 69, 220, 1965.*

7. Sposito, G., *The Surface Chemistry of Soils,* Oxford University Press, New York, 1984.

8. Parfitt, R. L., Fraser, A. R., Russell, J. D., and Farmer, V. C., Adsorption on hydrous oxides. II. Oxalate, benzoate and phosphate on gibbsite, J. *Soil Sci.,* 28, 40, 1977.

9. Smith, R. W. and Hem, J. D., Effect of aging on aluminum hydroxide complexes in dilute aqueous solutions, U.S. *Geol. Surv. Water-Supply Pup., 1827D,* Dl, 1972.

IO. McBride, M. B., Fraser, A. R., and McHardy, W. J., Cu^{2+} Interaction with microcrystalline gibbsite. Evidence for oriented chemisorbed copper ions, Clays *Clay Miner.,* 32, 12, 1984.

I 1. Peri, J. B. and Hannan, R. B., Surface hydroxyl groups on y-alumina, J. *Phys.* Chem., 64, 1526, 1960.

12. Kummert, R. and Stumm, W., The surface complexation of organic acids on hydrous γ-Al_2O_3, *J. Colloid Interface Sci., 75, 373, 1980.*

13. Yates, D. E. and Healy, T. W., The structure of the silica/electrolyte interface, J. *Colloid Interface Sci., 44, 9, 1976.*

14. Schoen, R. and Roberson, C. E., Structures of aluminum hydroxide and geochemical implications, *Am. Mineral., 5.5, 43, 1970.*

15. Hem, J. D., Aluminum hydroxide polymerization and synthesis of microcrystalline gibbsite in solutions near pH 5.0 (Abstr.), *EOS Trans.,* 67, 931, 1986.

16. Wefers, K. and Bell, G. M., Oxides and hydroxides of aluminum, Tech. Paper No. 19, Alcoa Research Laboratories, Alcoa Center, PA, 1972, 5 1.
17. Smit, W. and Holten, C. L. M., Zeta-potential and radiotracer adsorption measurements on EFG α-Al_2O_3 single crystals in NaBr solutions, J. *Colloid Interface Sci., 78,* 1, 1980.
18. de Boer, J. H., Fortuin, J. M. H., Lippens, B. C., and Meijs, W. H., Study of the nature of surfaces with polar molecules. II. The adsorption of water on aluminas, J. *Catal.,* 2, I, 1963.
19. Robie, R. A., Hemingway, B. S., and Fisher, J. R., Thermodynamic properties of minerals and related substances at 298.15 K and 1 bar (10^5 Pascals) pressure and at higher temperatures, U.S. Geol. *Surv. Bull.,* 1452, 1978.
20. Tanabe, K., *Solid Acids und Bases,* Academic Press, New York, 1970.
21. Hughes, T. R., White, H. M., and White, R. J., Bronsted and Lewis acid site concentrations in fluorided alumina from the infrared spectra of adsorbed pyridine species, J. *Catal.,* 13, 58, 1969.
22. Boehm, P., Acidic and basic properties of hydroxylated metal oxide surfaces, *Discuss. Faraday Soc., 52, 264, 197* 1.
23. Medema, J., van Bokhoven, J. J. G. M., and Kuiper, A. E. T., Adsorption of bases on γ-Al_2O_3, J. *Catal., 25, 238, 1972.*
24. Scokart, P. 0. and Rouxhet, P. G., Characterization of the basicity of oxides through the infrared study of pyrrole adsorption, J. Chem. Soc. *Faraday Trans. I, 76, 1476, 1980.*
25. Basila, M. R. and Kantner, T. R., The nature of the acidic sites on silica-alumina. A reevaluation of the relative adsorption coefficients of chemisorbed pyridine, J. Phys. Chem., 70, 1681, 1981.
26. Scokart, P. 0. and Rouxhet, P. G., Comparison of the acid-base properties of various oxides and chemically treated oxides, J. *Colloid Interface Sci., 86, 96, 1982.*
27. Peri, J. B., Infrared study of adsorption of ammonia on dry y-alumina, J. Phys. Chem.. 69, 231, 1965.
28. Parfitt, G. D. and Rochester C. H., Surface characterization: chemical, *Characterization of Powder Surfaces,* Academic Press, San Francisco, 1976, chap. 2.
29. Kiviat, F. E. and Petrakis, L., Surface acidity of transition metal modified aluminas. Infrared and nuclear magnetic resonance investigation of adsorbed pyridine, J. Phys. *Chem,* 77, 1232, 1973.
30. Dawson, W. H., Kaiser, S. W., Ellis, P. D., and Inners, R. R., Carbon-13 cross-polarization magic-angle-spinning NMR study of n-butylamine adsorbed on y-alumina: characterization of surface acid sites, J. *Am. Chem. Soc.,* 103, 678, 1981.
31. Peri, J. B., Infrared and gravimetric study of the surface hydration of y-alumina, J. *Phys. Chem., 69, 211, 1965.*
32. James, R. 0. and Parks, G. A., Characterization of aqueous colloids by their electrical double-layer and intrinsic surface chemical properties, in Surface *and Colloid Science,* Vol. *12,* Matijevic, E., Ed., Plenum Press, New York, 1982, I 19.
33. Healy, T. W. and White, L. R., Ionizable surface group models of aqueous interfaces, *Adv. Colloid Interface Sci., 9, 303, 1978.*
34. Overbeek, J. Th. G., Electrochemistry of the double layer, in *Colloid Science,* Vol. 1, Kruyt, H. R., Ed., Elsevier, Amsterdam, 1952, chap. 4.
35. Bockris, J. O'M. and Reddy, A. K. N., *Modern Electrochemistry* Vols. l and 2, Plenum Press, New York, 1970.
36. Sparnaay, M. J., *The Electrical Double Layer,* Pergamon Press, Elmsford, NY, 1972.
37. Hiemenz, P. C., *Principles of Colloid and Surface Chemistry,* Marcel Dekker, New York. 1977.

38. van Olphen, H., *An Introduction to Clay Colloid Chemistry,* 2nd ed., Wiley-Interscience, New York, 1977.
39. Sposito, G., Characterization of particle surface charge, in *Environmental Particles,* Vol. 1, Buffle, J. and van Leeuwen, H. P., Eds., Lewis Publishers, Chelsea, MI, 1992, chap. 7.
40. Hunter, R. J., *Zeta Potential in Colloid Science. Principles and Applications,* Academic Press, London, I98 l.
41. van Riemsdijk, W. H., Bolt, G. H., Koopal, L. K., and Blaakmeer, J., Electrolyte adsorption on heterogeneous surfaces: adsorption models, J. *Colloid Interface Sci., 109, 219, 1986.*
42. Napper, D. H. and Hunter, R. J., Hydrosols, in *Surface Chemistry and Colloids,* Kerker, M., Ed., (Vol. 7 of MPT Int. Rev. Science, Ser. 1, Physical Chemistry, Buckingham, A. D., Ed.), University Park Press, Baltimore, 1972, 241.
43. Wiese, G. R. and Healy, T. W., Coagulation and electrokinetic behavior of TiO_2 and Al_2O_3 colloidal dispersions, J. *Colloid Interface Sci., 5* 1, 427, 1975.
44. Tschapek, M., Wasowski, C., and Sanchez, R. M. T., The P.Z.C. and I.E.P. of γ-Al_2O_3 and TiO_2, J. *Electroanal. Chem., 74,* 167, 1976.
45. Sprycha, R., Electrical double layer at alumina/electrolyte interface. I. Surface charge and zeta potential, J. *Colloid Interface Sci., 127,* 1, 1989.
46. Thomas, F., Bottero, J. Y., and Cases, J. M., An experimental study of the adsorption mechanisms of aqueous organic acids on porous aluminas. II. Electrochemical modelling of salicylate adsorption, *Colloids Surf., 37, 281, 1989.*
47. Wood, R., Fornasiero, D., and Ralston, J., Electrochemistry of the boehmite-water interface, *Colloids Surf., 5* 1, 389, 1990.
48. Rakotonarivo, E., Bottero, J. Y., Thomas, F., Poirier, J. E., and Cases, J. M., Electrochemical modeling of freshly precipitated aluminum hydroxide-electrolyte interface, *Colloids Surf., 33, 191, 1988.*
49. Yopps, J. A. and Fuerstenau, D. W., The zero point of charge of alpha-alumina, J. *Colloid Sci.,* 19, 61, 1964.
50. Bleam, W. F. and McBride, M. B., Cluster formation versus isolated-site adsorption. A study of Mn(II) and Mg(II) adsorption on boehmite and goethite, J. *Colloid Interface Sci., 103, 124, 1985.*
5 I. Huang, C.-P., The surface acidity of hydrous solids, in *Adsorption* of *Inorganics at Solid-Liquid Interfaces,* Anderson, M. A. and Rubin, A. J., Eds., Ann Arbor Science, Ann Arbor, MI, 1981, chap. 5.
52. Davis, J. A., James, R. O., and Leckie, J. O., Surface ionization and complexation at the oxide/water interface. I. Computation of electrical double layer properties in simple electrolytes, J. *Colloid Interface Sci., 63, 480, 1978.*
53. Huang, C.-P. and Stumm, W., Specific adsorption of cations on hydrous γ-Al_2O_3, *J. Colloid Interface Sci., 43, 409, 1973.*
54. Kavanagh, B. V., Posner, A. M., and Quirk, J. P., Effect of polymer adsorption on the properties of the electrical double layer, *Faraday Discuss. Chem. Soc., 59, 242, 1975.*
55. Tewari, P. H. and McLean, A. W., Temperature dependence of point of zero charge of alumina and magnetite, J. *Colloid Interface Sci., 40, 267,* 1972.
56. Akratopulu, K. Ch., Vordonis, L., and Lycourghiotis, A., Effect of temperature on the point of zero charge and surface dissociation constants of aqueous suspensions of γ-Al_2O_3, J. *Chem. Soc. Faraday Trans. I, 82, 3697, 1986.*

57. Ahmed, S. M., Studies of the double layer at oxide-solution interface, J. Phys. Chem., 73, 3546, 1969.
58. Wnek, W. and Davies, R., An analysis of the dependence of the zeta potential and surface charge on surfactant concentration, ionic strength, and pH, J. *Colloid Interface Sci.*, 60, 361, 1977.
59. Smith, R. W., The State of Al(III) in Aqueous Solution and Adsorption of Hydrolysis Products on α-Al_2O_3, Ph.D. thesis, Stanford University, Palo Alto, CA, 1969.
60. May, H. M., Helmke, P. A., and Jackson, M. L., Gibbsite solubility and thermodynamic properties of hydroxy-aluminum ions in aqueous solution at 25°C, Geochim. Cos-*mochim. Acta*, 43, 861, 1979.
61. Bloom, P. R. and Weaver, R. M., Effect of removal of reactive surface material on the solubility of synthetic gibbsites, Clays *Cluy Miner.*, 30, 281, 1982.
62. Schulthess, C. P. and Sparks, D. L., Backtitration technique for proton isotherm modeling of oxide surfaces, *Soil Sci. Soc. Am. J.*, 50, 1046, 1986.
63. Hingston, F. J., Posner, A. M., and Quirk, J. P., Anion adsorption by goethite and gibbsite. I. The role of the proton in determining adsorption envelopes, J. Soil *Sci.*, 23, 177, 1972.
64. Ferris, A. P. and Jepson, W. B., The exchange capacities of kaolinite and the preparation of homoionic clays, *J. Colloid Interface Sci.*, 5 I, 245, 1975.
65. Breeuwsma, A. and Lyklema, J., Physical and chemical adsorption of ions in the electrical double layer on hematite (α-Fe_2O_3), *J. Colloid Interface Sci.*, 43, 437, 1973.
66. Foissy, A., M'Pandou, A., LaMarche, J. M., and Jaffrezic-Renault, N., Surface and diffuse-layer charge at the TiO_2-electrolyte interface, Colloids Surf:, 5, 363, 1982.
67. Sprycha, R., Attempt to estimate σ_β charge components on oxides from anion and cation adsorption measurements, J. *Colloid Interface Sci.*, 96, 550, 1983.
68. Shiao, S.-Y. and Meyer, R. E., Adsorption of inorganic ions on alumina from salt solutions: correlations of distribution coefficients with uptake of salt, *J. Inorg. Nucl. Chem.*, 43, 3301, 1981.
69. Sprycha, R., Surface charge and adsorption of background electrolyte ions at anatase/electrolyte interface, *J. Colloid Interface Sci.*, 102, 173, 1984.
70. Yates, D. E., Levine, S., and Healy, T. W., Site-binding model of the electrical double layer at the oxide/water interface, *J. Chem. Soc. Faraday Trans. I, 70, 1807, 1974.*
71. Bousse, L. and Meindl, J. S., Surface potential-pH characteristics in the theory of the oxide-electrolyte interface, in Geochemical *Processes at Mineral Surfaces*, Davis, J. A. and Hayes, K. F., Eds., ACS Symp. Ser. 323, American Chemical Society, Washington, D.C., 1986, chap. 5.
72. Bousse, L., de Rooij, N. F., and Bergveld, P., The influence of counter-ion adsorption on the ψ_0/pH characteristics of insulator surfaces, *Surf. Sci.*, 135, 479, 1983.
73. Bousse, L., de Rooij, N. F., and Bergveld, P., Operation of chemically sensitive field-effect sensors as a function of the insulator-electrolyte interface, IEEE *Trans. Electron Devices, 30, 1263, 1983.*
74. Stumm, W. and Morgan, J. J., *Aquatic Chemistry*, 2nd ed., John Wiley & Sons, New York, 1981.
75. Kurbatov, M. H., Wood, G. B., and Kurbatov, J. D., Isothermal adsorption of cobalt from dilute solutions, *J. Phys. Chem.*, 55, 1170, 1951.
76. Dugger, D. L., Stanton, J. H., Irby, B. N., McConnel, B. L., Cummings, W. W., and Maatman, R. W., The exchange of twenty metal ions with the weakly acidic silanol group of silica gel, *J. Phys. Chem.*, 68, 757, 1964.

77. Schindler, P. W., Surface complexes at oxide-water interfaces, in *Adsorption of Inorganics at Solid-Liquid Interfaces*, Anderson, M. A. and Rubin, A. J., Eds., Ann Arbor Science, Ann Arbor, MI, 1981, chap. 1.
78. Benjamin, M. M. and Leckie, J. O., Adsorption of metals at oxide interfaces: effects of the concentrations of adsorbate and competing metals, in *Contaminants und Sediments*, Vol. 2, Baker, R. A., Ed., Ann Arbor Science, Ann Arbor, MI, 1980, 305.
79. Tewari, P. H. and Lee, W., Adsorption of Co(I1) at the oxide/water interface, J. Colloid *Interface Sci.*, 52, 77, 1975.
80. McBride, M.B., Cu^{2+}-adsorption characteristics of aluminum hydroxide and oxyhydroxides, Clays *Clay Miner.*, 30, 21, 1982.
81. McBride, M. B., Sorption of copper(II) on aluminum hydroxide as affected by phosphate, Soil Sci. Soc. *Am. J.*, 49, 843, 1985.
82. Hachiya, K., Ashida, M., Sasaki, M., Kan, H., Inoue, T., and Yasunaga, T., Study of the kinetics of adsorption-desorption of Pb^{2+} on a γ-Al_2O_3 surface by means of relaxation techniques, J. Phys. Chem., 83, 1866, 1979.
83. Hachiya, K., Sasaki, M., Ikeda, T., Mikami, N., and Yasunaga, T., Static and kinetic studies of adsorption-desorption of metal ions on a γ-Al_2O_3 surface. II. Kinetic study by means of pressure-jump technique, J. Phys. Chem., 88, 27, 1984.
84. Hachiya, K., Sasaki, M., Saruta, Y., Mikami, N., and Yasunaga, T., Static and kinetic studies of adsorption-desorption of metal ions on a γ-Al_2O_3 surface. I. Static study of adsorption-desorption, J. Phys. Chem., 88, 23, 1984.
85. Yasunaga, T. and Ikeda, T., Adsorption-desorption kinetics at the metal-oxide-solution interface studied by relaxation methods, in *Geochemicul Processes at Mineral Surfaces*, Davis, J. A. and Hayes, K. F., Eds., ACS Symp. Ser. 323, American Chemical Society, Washington, D.C., 1986, chap. 12.
86. Benjamin, M. M., Effects of Competing Metals and Complexing Ligands on Trace Metals Adsorption at the Oxide/Solution Interface, Ph.D. thesis, Stanford University, Palo Alto, CA, 1979.
87. Wehrli, B., Ibric, S., and Stumm, W., Adsorption kinetics of vanadyl(IV) and chromium(III) to aluminum oxide: evidence for a two-step mechanism, *Colloids Surf.*, 51, 77, 1990.
88. Forbes, E. A., Posner, A. M., and Quirk, J. I?, The specific adsorption of divalent Cd, Co, Cu, Pb, and Zn on goethite, J. Soil *Sci.*, 27, 154, 1976.
89. Kinniburgh, D. G., The H^+/M^{2+} exchange stoichiometry of calcium and zinc adsorption on ferrihydrite, J. *Soil Sci., 34, 759, 1983.*
90. Hohl, H. and Stumm, W., Interaction of Pb^{2+} with hydrous γ-Al_2O_3, *J. Colloid Interface Sci., 55, 281, 1976.*
91. Honeyman, B. D. and Leckie, J. O., Macroscopic partitioning coefficients for metal ion adsorption, in *Geochemicul Processes at Mineral Surfaces*, Davis, J. A. and Hayes, K. F., Eds., ACS Symp. Ser. 323, American Chemical Society, Washington, D.C., 1986, chap. 9.
92. Davis, J. A. and Leckie, J. O., Surface ionization and complexation at the oxide/water interface. II. Surface properties of amorphous iron oxyhydroxide and adsorption of metal ions, *J. Colloid Interface Sci., 67, 90, 1978.*
93. Rudin, M. and Motschi, H., A molecular model for the structure of copper complexes on hydrous oxide surfaces: an ENDOR study of ternary Cu(II) complexes on δ-alumina, *J. Colloid Interface Sci., 98, 28.5, 1984.*

94. Möhl, W., Schweiger, A., and Motschi, H., Modes of phosphate binding to copper(B): investigations of the electron spin echo envelope modulation of complexes on surfaces and in solutions, *Inorg. Chem.*, 29, 1536, 1990.
95. Motschi, H. and Rudin, M., ^{27}Al ENDOR study of VO^{2+} adsorbed on &alumina, *Colloid Polym. Sci., 262, 579, 1984.*
96. Gessa, C., de Cherchi, M. L., Melis, P., Micera, G., and Strinna Erre, L., Anion-induced metal binding in amorphous aluminium hydroxide, *Colloids Surf.,* I I, *109, 1984.*
97. Micera, G., Dallocchio, R., Deiana, S., Gessa, C., Melis, P., and Premoli, A., Manganese(B) aluminium hydroxide interaction: an ESR study, *Colloids Surf.,* 17,395, 1986.
98. Chisholm-Brause, C. J., Hayes, K. F., Roe, A. L., Brown, G. E., Parks, G. A., and Leckie, J. O., Spectroscopic investigation of Pb(lI) complexes at the γ-Al_2O_3/water interface, *Geochim. Cosmochim. Acta, 54, 1897, 1990.*
99. Karthein, R., Motschi, H., Schweiger, A., Ibric, S., Sulzberger, B., and Stumm, W., Interactions of chromium(III) complexes with hydrous δ-Al_2O_3: rearrangements in the coordination sphere studied by electron spin resonance and electron spin-echo spectroscopies, *Inorg. Chem., 30,* 1606, 1991.
100. Vordonis, L., Spanos, N., Koutsoukos, P. G., and Lycourghiotis, A., Mechanism of adsorption of Co^{2+} and Ni^{2+} ions on the "pure and fluorinated y-alumina/electrolyte solution" interface, *Langmuir,* 8, 1736, 1992.
101. Baccini, P., Grieder, E., Stierli, R., and Goldberg, S., The influence of natural organic matter on the adsorption properties of mineral particles in lake water, *Schweiz. Z. Hydrol., 44, 99, 1982.*
102. Honeyman, B. D., Cation and Anion Adsorption at the Oxide/Solution Interface in Systems Containing Binary Mixtures of Adsorbents: An Investigation of the Concept of Adsorptive Additivity, Ph.D. thesis, Stanford University, Palo Alto, CA, 1984.
103. Shiao, S. -Y., Egozy, Y., and Meyer, R. E., Adsorption of Cs(I), Sr(II), Eu(III), Co(II) and Cd(II) by Al_2O_3, J. *Inorg. Nucl. Chem.,* 43, 3309, 1981.
104. Micera, G., Gessa, C., Melis, P., Premoli, A., Dallocchio, R., and Deiana, S., Zn(II) adsorption on aluminium hydroxide, Colloids *Surf., 17,* 389, 1986.
105. Elliott, H. A. and Huang, C. P., The adsorption characteristics of Cu(II) in the presence of chelating agents, J. *Colloid Interface Sci., 70, 29, 1979.*
106. Bowers, A. R. and Huang, C. I?, Adsorption characteristics of metal-EDTA complexes onto hydrous oxides, J. *Colloid Interface Sci.,* 110, *575, 1986.*
107. Bowers, A. R. and Huang, C. P., Role of Fe(III) in metal complex adsorption by hydrous solids, *Water Rex, 7, 757, 1987.*
108. Girvin, D. C., Gossman, P. L., and Bolton, H., Adsorption of aqueous cobalt ethylene diaminetetraacetate by δ-Al_2O_3, *Soil Sci. Soc.* Am. J., 57, 47, 1993.
109. Micera. G., Strinna Erre, L., and Dallocchio, R., Metal complex formation on the surface of amorphous aluminium hydroxide. I. Copper(II) complexes of glutamic and aspartic acids, *Colloids Surf., 28,* 147, 1987.
110. Micera, G. and Dallocchio, R., Metal complex formation on the surface of amorphous aluminum hydroxide. IV. Interaction of oxovanadium(IV) and vanadate(V) with aluminium hydroxide in the presence of succinic, malic and 2-mercaptosuccinic acids, *Colloids Surf., 34, 185, 1988.*
111. Micera, G., Strinna Erre, L., and Dallocchio, R., Metal complex formation on the surface of amorphous aluminium hydroxide. II. Copper(II) complexes with pyridinedicarboxylic acids, *Colloids Surf., 32, 237, 1988.*

112. Micera, G. and Dallocchio, R., Effect of the ligand structure on the formation of copper(II) complexes on the surface of amorphous aluminium hydroxide in the presence of 2,3-diaminopropionic and 2,4-diaminobutyric acids, Colloids Surf., 4.5, 167, 1990.
113. Micera, G., Strinna Erre, L., and Dallocchio, R., Metal complex formation on the surface of amorphous aluminium hydroxide. V. Copper(B) complexes with aluminium hydroxide in the presence of o-, m- and p-tyrosine and dopa, *Colloids Surf, 44, 237, 1990.*
114. Micera, G., Strinna Erre, L., and Dallocchio, R., Anchoring of copper(B)-dipeptide complexes to the surface of amorphous aluminium hydroxide, J. Chem. *Res. (S),* 234, 1992.
115 Xu, H., Ephraim, J., Ledin, A., and Allard, B., Effects of fulvic acid on the adsorption of Cd(II) on alumina, *Sci. Total Environ.,* 81/82, 653, 1989.
116. Davis, J. A., Complexation of trace metals by adsorbed natural organic matter, *Geochim. Cosmochim. Acta, 48, 679, 1984.*
117. Hingston, F. J., Posner, A. M., and Quirk, J. P., Competitive adsorption of negatively charged ligands on oxide surfaces, *Discuss. Faraday Soc., 52, 334, I97* 1.
118. Hingston, F. J., Posner, A. M., and Quirk, J. P., Anion adsorption by goethite and gibbsite. 11. Desorption of anions from hydrous oxide surfaces, J. *Soil Sci.,* 25, 16, 1974.
l 19. Huang, C. P., Adsorption of phosphate at the hydrous γ-Al_2O_3 electrolyte interface, *J.* Colloid *Interface Sci.,* 53, 178, 1975.
120. Kyle, J. H., Posner, A. M., and Quirk, J. P., Kinetics of isotopic exchange of phosphate adsorbed on gibbsite, *J. Soil Sci.,* 26, 32, 1975.
121. Davis, J. A. and Leckie, J. O., Surface ionization and complexation at the oxide/water interface. III. Adsorption of anions, *J. Colloid Interface Sci., 74, 32,* 1980.
122. Anderson, M. A., Ferguson, J. F., and Gavis, J., Arsenate adsorption on amorphous aluminum hydroxide, *J. Colloid Interface Sci., 54, 39* 1, 1976.
123. MacNaughton, M. G., Adsorption of chromium(VI) at the oxide/water interface, in *Biological Implications of Metals in the Environment,* Ducker, H. and Wildung, R. E., Eds., CONF-75029, National Technical Information Service, Springfield, VA, 1977, 240.
124. Anderson, M. A. and Malotky, D. T., The adsorption of protolyzable anions on hydrous oxides at the isoelectric pH, *J. Colloid Interface Sci.. 72, 413,* 1979.
125. Mikami, N., Sasaki, M., Hachiya, K., Astumian, R. D., Ikeda, T., and Yasunaga, T., Kinetics of the adsorption-desorption of phosphate on the γ-Al_2O_3 surface using the pressure-jump technique, *J. Phys. Chem., 87, 1454, 1983.*
126. Mikami, N., Sasaki, M., Kikuchi, T., and Yasunaga, T., Kinetics of adsorption-desorption of chromate on γ-Al_2O_3 surfaces using the pressure-jump technique, *J. Phys. Chem., 87, 5245, 1983.*
127. Hayes, K. F., Equilibrium, Spectroscopic, and Kinetic Studies of Ion Adsorption at the Oxide/Aqueous Interface, Ph.D. thesis, Stanford University, Palo Alto, CA, 1987.
128. Chen, Y.-S. R., Butler, J. N., and Stumm, W., Adsorption of phosphate on alumina and kaolinite from dilute aqueous solutions, *J. Colloid Interface Sci., 43, 42* I, 1973.
129. Kuo, S. and Lotse, E. G., Kinetics of phosphate adsorption and desorption by hematite and gibbsite, *Soil Sci.,* l 16, 400, 1974.
130. Rajan, S. S. S., Adsorption of selenite, phosphate and sulphate on hydrous alumina, *J.* Soil *Sci.,* 30, 709, 1979.

I3 1. Chen, Y.-S. R., Butler, J. N., and Stumm, W., Kinetic study of phosphate reaction with aluminum oxide and kaolinite, Environ. *Sci. Technol.,* 7, 327, 1973.
132. Helyar, K. R., Munns, D. N., and Burau, R. G., Adsorption of phosphate by gibbsite. I. Effects of neutral chloride salts of calcium, magnesium, sodium, and potassium, *J. Soil Sci.,* 27, 307, 1976.
133. van Riemsdijk, W. H., Weststrate, F. A., and Beek, J., Phosphates in soils treated with sewage water. III. Kinetic studies on the reaction of phosphate with aluminum compounds, *J. Environ. Qual., 6, 26,* 1977.
134. van Riemsdijk, W. H. and Lyklema, J., Reaction of phosphate with gibbsite $[Al(OH)_3]$ beyond the adsorption maximum, *J.* Colloid Interface *Sci.,* 76, 55, 1980.
135. van Riemsdijk, W. H. and Lyklema, J., The reaction of phosphate with aluminum hydroxide in relation with phosphate bonding in soils, Colloids Surf., 1, 33, 1980.
136. Lijklema, L., Interaction of orthophosphate with iron(III) and aluminum hydroxides, *Environ. Sci. Technol., 14, 537, 1980.*
137. Bolan, N. S., Barrow, N. J., and Posner, A. M., Describing the effect of time on sorption of phosphate by iron and aluminum hydroxides, *J. Soil Sci.,* 36, 187, 1985.
138. Sims, J. R. and Bingham, F. T., Retention of boron by layer silicates, sesquioxides, and soil materials. II. Sesquioxides, *Soil Sci. Soc.* Am. *Proc.,* 32, 364, 1968.
139. McPhail, M., Page, A. L., and Bingham, F. T., Adsorption interactions of monosilicic and boric acid on hydrous oxides of iron and aluminum, *Soil Sci. Soc.* Am. *Proc.,* 36, 510, 1972.
140. Choi, W.-W. and Chen, K. Y., Evaluation of boron removal by adsorption on solids, Environ. *Sci.* Technol., 13, 189, 1979.
141. Hingston, F. J. and Raupach, M., The reaction between monosilicic acid and aluminum hydroxide. I. Kinetics of adsorption of silicic acid by aluminum hydroxide, *Aust. J.* Soil *Res.,* 5, 295, 1967.
142. Adu-Wusu, K. and Wilcox, W. R., Kinetics of silicate reaction with gibbsite, *J.* Colloid *Interface Sci.,* 143, 127, 1991.
143. Choi, W.-W. and Chen, K. Y., The removal of fluoride from waters by adsorption, *J. Am. Water Works Assoc.,* 71, *562, 1979.*
144. Hao, 0. J. and Huang, C. P., Adsorption characteristics of fluoride onto hydrous alumina, *J. Environ. Eng.,* I 12, 1054, 1986.
145. Alvarez, R., Cramer, R. E., and Silva, J. A., Laser raman spectroscopy: a technique for studying adsorption on aluminum sesquioxide, gibbsite, *Soil Sci. Soc.* Am. *J.,* 40, 317, 1976.
146. Bleam, W. F., Pfeffer, P. E., Goldberg, S., Taylor, R. W., and Dudley, R., A ^{31}P solid-state nuclear magnetic resonance study of phosphate adsorption at the boehmite/aqueous solution interface, *Langmuir, 7, 1702,* 1991.
147. Jepson, W. B., Jeffs, D. G., and Ferris, A. P., The adsorption of silica on gibbsite and its relevance to the kaolinite surface, *J. Colloid Interface Sci., 55, 454, 1976.*
148. Alwitt, R. S., The point of zero charge of pseudoboehmite, *J. Colloid Interface Sci., 40, 195, 1972.*
149. Goldberg, S., Forster, H. S., and Heick, E. L., Boron adsorption mechanisms on oxides, clay minerals, and soils inferred from ionic strength effects, *Soil Sci. Soc.* Am. *J.,* 57, 704, 1993.
150. Adu-Wusu, K. and Wilcox, W. R., Sorption and desorption isotherms for silicate on gibbsite, *J. Colloid Interface Sci.,* 143, 139, 1991.
15 1. Muljadi, D., Posner, A. M., and Quirk, J. P., The mechanism of phosphate adsorption by kaolinite, gibbsite, and pseudoboehmite. III. The effect of temperature on adsorption, *J.* Soil *Sci.,* 17, 238, 1966.

152. Goldberg, S., Forster, H. S., and Heick, E. L., Temperature effects on boron adsorption by reference minerals and soils, *Soil Sci.*, 156, 316, 1993.
153. Helmy, A. K., de Bussetti, S. G., and Ferreiro, E. A., Sorption isotherms of mono- and divalent phosphate on hydrous Al oxides, *Colloids Surf., 58, 9,* 1991.
154. Xu, H., Allard, B., and Grimvall, A., Influence of pH and organic substance on the adsorption of As(V) on geologic materials, *Water Air Soil Pollut., 40, 293,* 1988.
155. Goldberg, S. and Glaubig, R. A., Boron and silicon adsorption on an aluminum oxide, *Soil Sci. Soc.* Am. J., 52, 87, 1988.
156. Violante, A., Colombo, C., and Buondonno, A., Competitive adsorption of phosphate and oxalate by aluminum oxides, Soil Sci. Soc. *Am. J., 55, 65,* 1991.
157. Xu, H., Allard, B., and Grimvall, A., Effects of acidification and natural organic materials on the mobility of arsenic in the environment, Water *Air Soil Pollut., 57-58, 269, 1991.*
158. Davis, J. A., Adsorption of natural dissolved organic matter at the oxide/water interface, *Geochim. Cosmochim. Acta, 46, 2381, 1982.*
159. McBride, M. B. and Wesselink, B., Chemisorption of catechol on gibbsite, boehmite, and amorphous alumina surfaces, *Environ. Sci. Technol., 22, 703, 1988.*
160. Davis, J. A. and Gloor, R., Adsorption of dissolved organics in lake water by aluminum oxide. Effect of molecular weight, *Environ. Sci.* Technol., 15, 1223, 1981.
161. Schulthess, C. P. and Huang, C. P., Humic and fulvic acid adsorption by silicon and aluminum oxide surfaces on clay minerals, Soil *Sci. Soc. Am. J., 55, 34,* 1991.
162. Tomaic, J. and Zutic, V., Humic material polydispersity in adsorption at hydrous alumina/seawater interface, J. Colloid *Interface Sci.,* 126, 482, 1988.
163. Zutic, V. and Tomaic, J., On the formation of organic coatings on marine particles: interactions of organic matter at hydrous alumina/seawater interfaces, Mar. *Chem., 23,* 51, 1988.
164. Parfitt, R. L., Farmer, V. C., and Russell, J. D., Adsorption on hydrous oxides. I. Oxalate and benzoate on gibbsite, J. Soil Sci., 28, 29, 1977.
165. Bowers, A. R. and Huang, C. P., Adsorption characteristics of polyacetic amino acids onto hydrous γ-Al_2O_3, *J. Colloid Interface Sci., 105, 197,* 1985.
166. Wakamatsu, T. and Fuerstenau, D. W., The effect of hydrocarbon chain length on the adsorption of sulfonates at the solid/water interface, in *Adsorption from Aqueous* Solution, ACS Advances in Chemistry Series 79, American Chemical Society, Washington, DC., 1968.
167. Bitting, D. and Harwell, J. H., Effects of counterions on surfactant surface aggregates at the alumina/aqueous solution interface, *Langmuir,* 3, 500, 1987.
168. Han, K. N., Healy, T. W., and Fuerstenau, D. W., The mechanism of adsorption of fatty acids and other surfactants at the oxide-water interface, J. *Colloid Interface Sci., 44, 407, 1973.*
169. Thomas, F., Bottero, J. Y., and Cases, J. M., An experimental study of the adsorption mechanisms of aqueous organic acids on porous aluminas. 1. The porosity of the adsorbent: a determining factor for the adsorption mechanisms, *Colloids Surf, 37, 269, 1989.*
170. Hsu, P. H., Formation of gibbsite from aging hydroxy-alumina solutions, *Soil Sci. Soc. Am. Proc.,* 30, 173, 1966.
171. Vermeulen, A. C., Geus, J. W., Stol, R. J., and de Bruyn, P. L., Hydrolysis-precipitation studies of aluminum(III) solutions. I. Titration of acidified aluminum nitrate solutions, *J. Colloid Interface Sci., 5* I, *449,* 1975.
172. Stol, R. J., van Helden, A. K., and de Bruyn, P. L., Hydrolysis-precipitation studies of aluminum(III) solutions. II. A kinetic study and model, J. *Colloid Interface Sci., 57,* 115, *1976.*

173. Parthasarathy, N. and Buffle, J., Study of polymeric aluminum(III) hydroxide solutions for application of waste water treatment: properties of the polymer and optimal conditions of preparation, *Water Res.*, 19, 25, 1985.
174. Hem, J. D., Kinetics of dissolution and structure of aluminum hydroxide polymers, in *Leaching and Diffusion in Rocks and Their Weathering Products.* Augustuthis, S. S., Ed., Theophrastus Publications S.A., Athens, 1983, 51.
175. Hem, J. D. and Roberson, C. E., Aluminum hydrolysis reactions and products in mildly acidic aqueous systems, in *Chemical Modeling of Aqueous Systems,* Vol. 2, Melchior, D. C. and Bassett, R. L., Eds., ACS Symp. Ser. 416, American Chemical Society, Washington, D.C., 1990, chap. 33.
176. van Straten, H. A., Holtkamp, B. T. W., and de Bruyn, P. L., Precipitation from supersaturated aluminate solutions. I. Nucleation and growth of solid phases at room temperature, J. *Colloid Interface Sci., 98, 342, 1984.*
177. van Straten, H. A. and de Bruyn, P. L., Precipitation from supersaturated aluminate solutions. II. Role of temperature, J. *Colloid Interface Sci., 102, 260, 1984.*
178. Smith, R. W., Relations among equilibrium and nonequilibrium aqueous species of aluminum hydroxide complexes, in *Nonequilibrium Systems in Natural Water Chemistry,* Advances in Chemistry Series 106, American Chemical Society, Washington, D.C., 1971, 250.
179. Violante, A. and Huang, P. M., Influence of inorganic and organic ligands on the formation of aluminum hydroxides and oxyhydroxides, *Clays Clay Miner,* 33, 181, 1985.
180. Hsu, I? H., Effect of phosphate and silicate on the crystallization of gibbsite from OH-AI solutions, *Soil Sci.,* 127, 219, 1979.
181. Kwong, N.-K. K. F. and Huang, P. M., The relative influence of low-molecular-weight, complexing organic acids on the hydrolysis and precipitation of aluminum, *Soil Sci.,* 128, 337, 1979.
182. Violante, A. and Violante, P., Influence of pH, concentration, and chelating power of organic anions on the synthesis of aluminum hydroxides and oxyhydroxides, *Clays Clay Miner,* 28, 425, 1980.
183. Kodama, H. and Schnitzer, M., Effect of fulvic acid on the crystallization of aluminum hydroxides, *Geoderma, 24, 195, 1980.*
184. van Straten, H. A., Schoonen, A. A., Verheul, R. C. S., and de Bruyn, P. L., Precipitation from supersaturated aluminate solutions. IV. Influence of citrate ions, J. *Colloid Interface Sci., 5* 1, 449, 1985.
185. Zutic, V. and Stumm, W., Effect of organic acids and fluoride on the dissolution kinetics of hydrous alumina. A mode1 study using the rotating disc electrode, *Geochim. Cosmochim. Acta, 48, 1493, 1984.*
186. Furrer, G. and Stumm, W., The coordination chemistry of weathering. I. Dissolution kinetics of δ-Al_2O_3 and BeO, *Geochim. Cosmochim. Acta, 50,* 1847, 1986.
187. Dzombak, D. A. and Morel, F. M. M., Adsorption of inorganic pollutants in aquatic systems, J. *Hydraul. Eng.,* I 13, 430, 1987.
188. Sposito, G., On the surface complexation model of the oxide-aqueous solution interface, J. *Colloid Interface Sci., 9* 1, 329, 1983.
189. Schindler, P. W. and Gamsjäer, H., Acid-base reactions of the TiO_2 (anatase)-water interface and the point of zero charge of TiO_2 suspensions, *Kolloid-Z. Z. Polym., 250, 759, 1972.*
190. Schindler, P. W., Fürst, B., Dick, R., and Wolf, P. U., Ligand properties of surface silanol groups. I. Surface complex formation with Fe'+, Cu^{2+}, Cd^{2+}, and Pb^{2+}, J. *Colloid Interface Sci., 55, 469, 1976.*

191. Stumm, W., Hohl, H., and Dalang, F., Interaction of metal ions with hydrous oxide surfaces, *Crouticu Chem. Acta, 48, 491,* 1976.
192. Stumm, W., Kummert, R., and Sigg, L., A ligand exchange model for the adsorption of inorganic and organic ligands at hydrous oxide interfaces, *Crouticu Chem. Acta, 53, 291, 1980.*
193. Hohl, H., Sigg, L., and Stumm, W., Characterization of surface chemical properties of oxides in natural waters, in *Particulates in Water,* Kavanagh, M. C. and Leckie, J. O., Eds., ACS Advances in Chemistry Series 189, American Chemical Society, Washington, D.C., 1980, chap. 1.
194. Blesa, M. A., Maroto, A. J. G., and Regazzoni, A. E., Boric acid adsorption on magnetite and zirconium dioxide, J. *Colloid Interface Sci.,* 99, 32, 1984.
195. Hayes, K. F. and Leckie, J. O., Mechanism of lead ion adsorption at the goethite-water interface, in *Geochemical Processes at Mineral Surfaces,* Davis, J. A. and Hayes, K. F., Eds., ACS Symp. Ser. 323, American Chemical Society, Washington, D.C., 1986, chap. 7.
196. Goldberg, S., Use of surface complexation models in soil chemical systems, *Adv. Agron.,* 47, 233, 1992.
197. Sprycha, R., Electrical double layer at alumina/electrolyte interface. II. Adsorption of supporting electrolyte ions, J. *Colloid Interface Sci.,* 127, 12, 1989.
198. Bolt, G. H. and van Riemsdijk, W. H., Ion adsorption on inorganic variable charge constituents, in Soil *Chemistry, Purt B, Physicochemical Methods,* Bolt, G. H., Ed., Elsevier, Amsterdam, 1982, 459.
199. van Riemsdijk, W. H., de Wit, J. C. M., Koopal, L. K., and Bolt, G. H., Metal ion adsorption on heterogeneous surfaces: adsorption models, J. Colloid *Interface Sci.,* 116, 51 I, 1987.
200. Hiemstra, T., van Riemsdijk, W. H., and Bruggenwert, M. G. M., Proton adsorption mechanism at the gibbsite and aluminium oxide solid/solution interface, *Netherlands J. Agric. Sci., 35, 281, 1987.*
201. van Riemsdijk, W. H. and van der Zee, S. E. A. T. M., Comparison of models for adsorption, solid solution and surface precipitation, in *Interactions at the Soil Colloid-Soil Solution Interface,* Bolt, G. H., Ed., Kluwer Academic Publishers, Netherlands, 1991, 241.
202. Hiemstra, T., van Riemsdijk, W. H., and Bolt, G. H., Multisite proton adsorption modeling at the solid/solution interface of (hydr)oxides: a new approach. 1. Model description and evaluation of intrinsic reaction constants, J. *Colloid Interface Sci., 133, 91, 1989.*
203. Hiemstra, T., de Wit, J. C. M., and van Riemsdijk, W. H., Multisite proton adsorption modeling at the solid/solution interface of (hydr)oxides: a new approach. II. Application to various important (hydr)oxides, J. Colloid *Interface Sci.,* 133, 105, 1989.
204. Stumm, W. and Wollast, R., Coordination chemistry of weathering: kinetics of the surface-controlled dissolution of oxide minerals, *Rev. Geophys.,* 28, 53, 1990.
205. Schulthess, C. P. and Sparks, D. L., A critical assessment of surface adsorption models, Soil Sci. Soc. *Am. J., 52, 92, 1988.*
206. Anderson, P R. and Benjamin, M. M., Modeling adsorption in aluminum-iron binary oxide suspensions, *Environ. Sci. Technol., 24,* 1586, 1990.
207. Goldberg, S. and Glaubig, R. A., Effect of saturating cation, pH, and aluminum and iron oxide on the flocculation of kaolinite and montmorillonite, Clays Clay *Miner., 35, 220, 1987.*

208. Robinson, M., Pask, J. A., and Fuerstenau, D. W., Surface charge of alumina and magnesia in aqueous media, J. *Am. Ceramic Soc.,* 47, 5 16, 1964.
209. Parks, G. A., The isoelectric points of solid oxides, solid hydroxides, and aqueous hydroxo complex systems, Chem. *Rev.,* 6.5, 177, 1965.
210. Sadek, H., Helmy, A. K., Sabet, V. M., and Tadros, T. H. F., Adsorption of potential-determining ions at the aluminium oxide-aqueous interface and the point of zero charge, *J. Electronal. Chem., 27, 257,* 1970.
211. Schwarz, J. A., Driscoll, C. T., and Bhanot, A. K., The zero point of charge of silica-alumina oxide suspensions, *J. Colloid Interface Sci., 97, 55,* 1984.
212. Feldkamp, J. R., Shah, D. N., Meyer, S. L., White, J. L., and Hem, S. L., Effect of adsorbed carbonate on surface charge characteristics and physical properties of aluminum hydroxide gel, *J. Pharm. Sci.,* 70, 638, 1981.
213 Beyrouty, C. A., van Scoyoc, G. E., and Feldkamp, J. R., Evidence supporting specific adsorption of boron on synthetic aluminum hydroxides, Soil Sci. Soc. *Am. J.,* 48, 284, 1984.
214. Cambier, P. and Sposito, G., Adsorption of citric acid by synthetic pseudoboehmite, Clays Clay *Miner., 39, 369,* 1991.
215. Benjamin, M. M. and Leckie, J. O., Effects of complexation by Cl, SO_4, and S_2O_3 on adsorption behavior of Cd on oxide surfaces, *Environ. Sci. Technol., 16, 162, 1982.*
216. Schulthess, C. P. and Huang, C. P., Adsorption of heavy metals by silicon and aluminum oxide surfaces on clay minerals, *Soil Sci. Soc. Am. J., 54, 679, 1990.*
217. James, R. 0. and MacNaughton, M. G., The adsorption of aqueous heavy metals on inorganic materials, *Geochim. Cosmochim. Acta, 41,* 1549, 1977.
218. Alvarez, R., Fadley, C. S., and Silva, J. A., Silicate and phosphate adsorption on gibbsite studied by x-ray photoelectron spectroscopy angular distributions, Soil *Sci. Soc. Am. J.,* 44, 422, 1980.
219. Okazaki, M., Takamidoh, K., and Yamane, I., Adsorption of heavy metal cations on hydrated oxides and oxides of iron and aluminum with different crystallinities, *Soil Sci. Plant Nutr., 32, 523, 1986.*
220. Pavlova, V. and Sigg, L., Adsorption of trace metals on aluminium oxide: a simulation of processes in freshwater systems by close approximation to natural conditions, *Water Res., 12, 1571, 1988.*
221. Anderson, P. R. and Benjamin, M. M., Surface and bulk characteristics of binary oxide suspensions, *Environ. Sci. Technol., 24, 692,* 1990.
222. Kinniburgh, D. G., Syers, J. K., and Jackson, M. L., Specific adsorption of trace amounts of calcium and strontium by hydrous oxides of iron and aluminum, Soil *Sci. Soc.* Ant. *J.,* 39, 464, 1975.
223. Kinniburgh, D. G., Jackson, M. L., and Syers, J. K., Adsorption of alkaline earth, transition, and heavy metal cations by hydrous oxide gels of iron and aluminum, *Soil Sci. Soc. Am. J., 40, 796, 1976.*
224. Kinniburgh, D. G., Sridhar, R., and Jackson, M. L., Specific adsorption of zinc and cadmium by iron and aluminum hydrous oxides, in *Biological Implications of Metals in the Environment,* Ducker, H. and Wildung, R. E., Eds., CONF-75029, National Technical Information Service, Springfield, VA, 1977.
225. McBride, M. B., Retention of Cu^{2+}, Ca^{2+} Mg^{2+}, and Mn^{2+} by amorphous alumina, Soil *Sci. Soc.* Am. *J.,* 42, 27, 1978.
226. Goldberg, S. and Glaubig, R. A., Boron adsorption on aluminum and iron oxide minerals, Soil Sci. Soc. Am. *J.,* 49, 1374, 1985.

227. Ferreiro, E. A., Helmy, A. K., and de Bussetti, S. G., Molybdate sorption by oxides of aluminium and iron, Z. Pflanzenernaehr. *Bodenk., 148, 559, 1985.*

228. Peinemann, N. and Helmy, A. K., Sorption of phosphate by hydrous oxides of aluminium and iron, J. *Electroanal. Chem., 78, 325, 1977.*

229. Farrah, H., Slavek, J., and Pickering, W. F., Fluoride interactions with hydrous aluminium oxides and alumina, *Aust. J. Soil Res.,* 25, 55, 1987.

230. Muljadi, D., Posner, A. M., and Quirk, J. P., The mechanism **of** phosphate adsorption by kaolinite, gibbsite, and pseudoboehmite. I. The isotherms and the effect of pH on adsorption, J. *Soil Sci.,* 17, 212, 1966.

231. Alvarez, R., Fadley, C. S., Silva, J. A., and Uehara, G., A study of silicate adsorption on gibbsite ($Al(OH)_3$) by x-ray photoelectron spectroscopy (XPS), *Soil Sci. Soc. Am. J.,* 40, 615, 1976.

232. Okazaki, M., Sakaidani, K., Saigusa, T., and Sakaida, N., Ligand exchange of oxyanions on synthetic hydrated oxides of iron and aluminium, *Soil Sci. Plant Nutr.,* 35, 337, 1989.

233. Beckwith, R. S. and Reeve, R., Studies on soluble silica in soils. I. The sorption of silicic acid by soils and minerals, *Aust. J. Soil Res.,* 1, 157, 1963.

234. Serna, C. J., White, J. L., and Hem, S. L., Anion-aluminum hydroxide gel interactions, *Soil Sci. Soc.* Am. J., 41, 1009, 1977.

235. Nanzyo, M., Diffuse reflectance infrared spectra of phosphate sorbed on alumina gel, J. *Soil Sci.,* 35, 63, 1984.

236. Gulledge, J. H. and O'Connor, J. T., Removal of As(V) from water by adsorption on aluminum and ferric hydroxides, J. *Am. Water Works Assoc., 65, 548, 1973.*

237. Stone, A. T., Torrents, A., Smolen, J., Vasudevan, D., and Hadley, J., Adsorption of organic compounds possessing ligand donor groups at the oxide/water interface, *Environ. Sci. Technol., 27, 895, 1993.*

238. Denoyel, R., Rouquerol, F., and Rouquerol J., Adsorption of anionic surfactants on alumina: complementarity of the information provided by batch and liquid flow microcalorimetry, *Colloids Surf, 37, 295, 1989.*

239. Denoyel, R. and Rouquerol, J., Thermodynamic (including microcalorimetry) study of the adsorption of nonionic and anionic surfactants onto silica, kaolin, and alumina, *J. Colloid Interface Sci., 143, 555, 1991.*

240. Jain, V. K., Mundhara, G. L., and Mishra, R. K., Sorption-desorption studies on alumina pretreated with acids. I. The anionic dye orange II, Surf. Technol., 26, 295, 1985.

241. Viswanathan, K. V. and Somasundaran, P., Adsorption of ethoxylated sulfonates on kaolinite and alumina, Colloids Surf., 26, 19, 1987.

242. Mishra, R. K., Mundhara, G. L., and Tiwari, J. S., Sorption-desorption studies of anionic dyes on alumina pretreated with acids, J. *Colloid Interface Sci., 129,41, 1989.*

243. Schulthess, C. P. and McCarthy, J. F., Competitive adsorption of aqueous carbonic and acetic acids by an aluminum oxide, *Soil Sci. Soc. Am. J.,* 54, 688, 1990.

244. Li, C., Yu, X., and Somasundaran, P., Effect of a comb-like amphiphilic polymer on the stability of alumina dispersions, *Colloids Surf., 69,* 155, 1992.

245. Parfitt, R. L., Fraser, A. R., and Farmer, V. C., Adsorption of hydrous oxides. 111. Fulvic acid and humic acid on goethite, gibbsite and imogolite, J. *Soil Sci..* 28, 289, 1977.

246. Kung, K.-H. S. and McBride, M. B., Bonding of chlorophenols on iron and aluminum oxides, *Environ. Sci. Technol., 25, 702,* 1991.

247. de Bussetti, S. G., Ferreiro, E. A., and Helmy, A. K., Adsorption of l,10-phenanthroline by some clays and oxides, *Clays Clay Miner.*, 28, 149, 1980.
248. Ferreiro, E. A., de Bussetti, S. G., and Helmy, A. K., Sorption of 2,2'-bipyridene on clays and oxides, Z. *Pflanzenernaehr. Bodenk.*, *146, 369, 1983.*
249. Helmy, A. K., de Bussetti, S. G., and Ferreiro, E. A., Adsorption of quinoline from aqueous solutions by some clays and oxides, Clays Clay Miner., 31, 29, 1983.
250. Rakotonarivo, E., Bottero, J. Y., and Cases, J. M., Study of the adsorption of long chain alkyl-sulfonates from aqueous solutions on aluminum hydroxide gels, *Colloids Surf., 9, 273, 1984.*
251. Rakotonarivo. E., Bottero, J. Y., Cases, J. M., and Leprince, A., Study of the adsorption of long chain sodium soaps from aqueous solutions on aluminum hydroxide gels, *Colloids Surf., 16, 153, 1985.*
252. Ferreiro, E. A., de Bussetti, S. G., and Helmy, A. K., Sorption of 8-hydroxyquinoline by some clays and oxides, *Clays Clay Miner.*, 36, 61, 1988.
253. Micera, G., Strinna Erre, L., and Dallocchio, R., Metal complex formation on the surface of amorphous aluminium hydroxide. III. Copper(B) complexes of o-phospho-L-serine and o-phospho-t-tyrosine, *Colloids Surf., 32, 249, 1988.*
254. Westall, J. and Hohl, H., A comparison of electrostatic models for the oxide/solution interface, *Adv. Colloid Interface Sci., 12, 265, 1980.*
255. Goldberg, S. and Sposito, G., A chemical model of phosphate adsorption by soils. I. Reference oxide minerals, Soil *Sci. Soc. Am. J.*, 48, 772, 1984.
256. Hayes, K. F., Redden, G., Ela, W., and Leckie, J. O., Surface complexation models: an evaluation of model parameterestimation using FJTEQL and oxide mineral titration data, *J. Colloid Interface Sci., 142, 448, 1991.*
257. Goldberg, S., Chemical modeling of specific anion adsorption on oxides, clay minerals, and soils, ENVIROSOFT 86, CML Publications, Ashurst, Southampton, UK, 1986, 671.
258. Goldberg, S., Chemical modeling of arsenate adsorption on aluminum and iron oxide minerals, *Soil Sci. Soc. Am. J., 50, 154, 1986.*
259. Pulfer, K., Schindler, P. W., Westall, J. C., and Grauer, R., Kinetics and mechanism of dissolution of bayerite (γ-$Al(OH)_3$) in HNO_3-HF solutions at 298.2 K, *J. Colloid Interface Sci.*, 101, 554, 1984.
260. Ainsworth, C. C., Girvin, D. C., Zachara, J. M., and Smith. S. C., Chromate adsorption on goethite: effects of aluminum substitution, *Soil Sci. Soc. Am. J.. 53, 41 I, 1989.*